JAERI-M
86-184

CROSS FLOW RESISTANCE IN AIR-WATER TWO-PHASE FLOW IN ROD BUNDLE

January 1987

Takamichi IWAMURA, Hiromichi ADACHI
and Makoto SOBAJIMA

日本原子力研究所
Japan Atomic Energy Research Institute

JAERI-Mレポートは，日本原子力研究所が不定期に公刊している研究報告書です。
入手の問合わせは，日本原子力研究所技術情報部情報資料課（〒319-11茨城県那珂郡東海村）あて，お申しこしください。なお，このほかに財団法人原子力弘済会資料センター（〒319-11 茨城県那珂郡東海村日本原子力研究所内）で複写による実費頒布をおこなっております。

JAERI-M reports are issued irregularly.
Inquiries about availability of the reports should be addressed to Information Division Department of Technical Information, Japan Atomic Energy Research Institute, Tokai-mura, Naka-gun, Ibaraki-ken 319-11, Japan.

編集兼発行　日本原子力研究所
印　　刷　いばらき印刷㈱

JAERI-M 86-184

Cross Flow Resistance in Air-Water Two-Phase Flow in Rod Bundle

Takamichi IWAMURA, Hiromichi ADACHI
and Makoto SOBAJIMA

Department of Reactor Safety Research
Tokai Research Establishment,
Japan Atomic Energy Research Institute

Tokai-mura, Naka-gun, Ibaraki-ken

(Received December 10, 1986)

In order to evaluate the cross flow rate during the reflood phase of a PWR-LOCA, a cross flow resistance of fuel rod bundle was experimentally obtained in an air-water two-phase flow in a rod bundle. The experimental ranges are: cross flow velocity at the gap between rods at the inlet and outlet sides of the bundle 0.224 - 2.99 m/s, vertical superficial water velocity 0.025 - 0.248 m/s, and void fraction 0 - 0.34. The air cross flow rate was small in comparison to the air up-flow rate. The cross flow resistance in the two-phase flow was much higher than that in a single-phase water flow. The cross flow resistance increased with the void fraction and decreased with the cross flow velocity up to a certain void fraction (critical void fraction). A correlation of the cross flow resistance was proposed for the void fraction range below the critical void fraction as a function of the void fraction and the cross flow Reynolds number. The critical void fraction increased with the cross flow and vertical water velocity. Above the critical void fraction, on the contrary, the cross flow resistance decreased with the void fraction. The cross flow attack angle against the bundle lattice had little effect on the two-phase cross flow resistance.

Keywords: Cross Flow Resistance, Two-phase Flow, Two-dimensional Effect, Reflood, LOCA, Reactor Safety, Void Fraction

---

The work was performed under contract with the Atomic Energy Bureau of Scince and Technology Agency of Japan

JAERI－M 86－184

バンドル内空気－水二相流中での横流れ抵抗係数

日本原子力研究所東海研究所原子炉安全工学部
岩村　公道・安達　公道・傍島　　真

（1986年12月10日受理）

PWR－LOCA時再冠水過程での横流れ流量を評価するため，空気－水二相流下での燃料集合体横流れ抵抗係数を実験的に求めた。実験範囲は，バンドル入口及び出口でのロッド間ギャップにおける横流れ流速0.224～2.99m／s，見かけの垂直水流速0.025～0.248m／s，およびボイド率0～0.34である。空気の横流れ流量は空気の上向き流量に比べて小さかった。二相流中での横流れ抵抗係数は水単相流中よりも大きく，あるボイド率（限界ボイド率）以下では，ボイド率上昇又は横流れ流速減少に伴って増加した。この領域での横流れ抵抗係数をボイド率及び横流れレイノルズ数の関数として表示する相関式を提案した。限界ボイド率は，横流れ及び垂直水流速の増大に伴い増加した。この限界ボイド率以上では，横流れ抵抗係数は逆にボイド率増加と共に減少した。また，二相流横流れ抵抗係数に及ぼす，横流れとバンドル格子の相対角度の影響は小さかった。

東海研究所：〒319－11 茨城県那珂郡東海村白方字白根2－4

本報告は，電源開発促進対策特別会計法に基づき，科学技術庁からの受託によって行なった研究の成果である。

Contents

1. INTRODUCTION 1
2. TEST FACILLITY 3
2.1 Test Facility 3
2.2 Instrumentation 4
3. TEST RESULTS AND DISCUSSIONS 11
3.1 Two-Phase Flow Behavior in Rod Bundle 11
3.2 Cross Flow Resistance in Two-Phase Flow 12
3.2.1 Calculation Method 12
3.2.2 Cross Flow Expansion Factor 15
3.2.3 Cross Flow Resistance in Two-Phase Flow 15
3.3 Correlation of Cross Flow Resistance in Two-Phase Flow 17
3.4 Effect of Cross Flow Angle on Cross Flow Resistance 18
3.4.1 Test Conditions 18
3.4.2 Cross Flow Resistance for Rod Arrangement with Different Angle 18
3.4.3 Horizontal Differential Pressure in Single-Phase Water Cross Flow 19
3.4.4 Cross Flow Resistance in Two-Phase Flow 20
4. CONCLUSIONS 38
ACKNOWLEDGEMENT 39
NOMENCLATURE 40
REFERENCES 42
APPENDIX TEST RESULTS 43

目　　次

1. 序　論 …… 1
2. 試験装置 …… 3
2.1 試験装置 …… 3
2.2 計　測 …… 4
3. 試験結果と検討 …… 11
3.1 ロッドバンドル内二相流挙動 …… 11
3.2 二相流内横流れ抵抗係数 …… 12
3.2.1 計算方法 …… 12
3.2.2 横流れ拡大係数 …… 15
3.2.3 二相流内横流れ抵抗係数 …… 15
3.3 二相流内横流れ抵抗係数相関式 …… 17
3.4 横流れ角度が抵抗係数に及ぼす効果 …… 18
3.4.1 試験条件 …… 18
3.4.2 異なる角度のロッド配列に対する抵抗係数 …… 18
3.4.3 水単相横流れにおける水平方向差圧 …… 19
3.4.4 二相流内横流れ抵抗係数 …… 20
4. 結　論 …… 38

謝　辞 …… 39
記号表 …… 40
参考文献 …… 42
付録　試験結果 …… 43

List of Tables

Table 3-1 Test conditions of two-phase cross flow experiments in Test section A

Table 3-2 Test conditions of two-phase cross flow experiments in Test sections B and C

Table A-1 Single-phase cross flow test results

Table A-2 Two-phase cross flow test results (H = 30 mm)

Table A-3 Two-phase cross flow test results (H = 60 mm)

Table A-4 Two-phase cross flow test results (H = 120 mm)

Table A-5 Two-phase cross flow test results (H = 120 mm, ψ = 60°)

Table A-6 Two-phase cross flow test results (H = 120 mm, ψ = 45°)

List of Figures

Fig. 2-1 Schematic diagram of cross flow test facility

Fig. 2-2 Test section

Fig. 2-3 Configurations of spacers

Fig. 2-4 Variable slit

Fig. 2-5 Arrangement of rods in three test sections with different cross flow attack angles

Fig. 2-6 Location and dimension of pressure tap

Fig. 3-1 Horizontal distribution of void fractions

Fig. 3-2 Examples of horizontal and vertical differential pressure transients

Fig. 3-3 Single-phase cross flow resistance vs. cross flow velocity

Fig. 3-4 Comparison of cross flow resistances obtained from two assumptions: no air phase at gap between rods and homogeneous two-phase mixture

Fig. 3-5 Horizontal differential pressure vs. cross flow velocity without flow expansion in single-phase water flow

Fig. 3-6 Cross flow expansion factor vs. cross flow velocity without flow expansion in single-phase water flow

Fig. 3-7 Measurement locations of horizontal and vertical differential pressure

Fig. 3-8 Cross flow resistance vs. void fraction
(H = 30 mm, $Q_{\ell h}$ = 50 ℓ/min)

Fig. 3-9 Cross flow resistance vs. void fraction
(H = 30 mm, $Q_{\ell h}$ = 100 ℓ/min)
Fig. 3-10 Cross flow resistance vs. void fraction
(H = 60 mm, $Q_{\ell h}$ = 30 ℓ/min)
Fig. 3-11 Cross flow resistance vs. void fraction
(H = 60 mm, $Q_{\ell h}$ = 50 ℓ/min)
Fig. 3-12 Cross flow resistance vs. void fraction
(H = 60 mm, $Q_{\ell h}$ = 75 ℓ/min)
Fig. 3-13 Cross flow resistance vs. void fraction
(H = 60 mm, $Q_{\ell h}$ = 1000 ℓ/min)
Fig. 3-14 Cross flow resistance vs. void fraction
(H = 60 mm, $Q_{\ell h}$ = 150 ℓ/min)
Fig. 3-15 Cross flow resistance vs. void fraction
(H = 120 mm, $Q_{\ell h}$ = 30 ℓ/min)
Fig. 3-16 Cross flow resistance vs. void fraction
(H = 120 mm, $Q_{\ell h}$ = 50 ℓ/min)
Fig. 3-17 Cross flow resistance vs. void fraction
(H = 120 mm, $Q_{\ell h}$ = 75 ℓ/min)
Fig. 3-18 Cross flow resistance vs. void fraction
(H = 120 mm, $Q_{\ell h}$ = 100 ℓ/min)
Fig. 3-19 Cross flow resistance vs. void fraction
(H = 120 mm, $Q_{\ell h}$ = 150 ℓ/min)
Fig. 3-20 Relation between cross flow resistance devided by void fraction and cross flow Reynolds number
Fig. 3-21 Applicable ranges of void fraction and cross flow Reynolds number for cross flow resistance correlation
Fig. 3-22 Horizontal differential pressure in single-phase flow vs. cross flow velocity at slit in Test Sections A, B and C (attack angles: 90°, 60° and 45°)
Fig. 3-23 Ratio of calculated horizontal differential pressure in single-phase cross flow between Test Sections C and A (attack angles: 45° and 90°) vs. cross flow Reynolds number
Fig. 3-24 Cross flow resistance perunit length in Test Sections A, B and C vs. void fraction
($Q_{\ell h}$ = 50 ℓ/min)

Fig. 3-25 Cross flow resistanve per unit length in Test Sections A, B and C vs. void fraction ($Q_{\ell h}$ = 100 ℓ/min)

List of Photographs

Photo. 3-1 Two-phase flow pattern in rod bundle ($V_{\ell ho}$ = 0.373 m/s, $V_{\ell v}$ = 0.0248 m/s)
Photo. 3-2 Two-phase flow pattern in rod bundle ($V_{\ell ho}$ = 0.747 m/s, $V_{\ell v}$ = 0.0248 m/s)

1. INTRODUCTION

In a large pressurized water reactor (PWR) with a nonuniform radial power distribution, the two-phase flow during the reflood phase of a loss-of-coolant accident (LOCA) is considered to concentrate in the higher power bundles because steam generation rate and flow rate are higher in those bundles and a natural convection is induced.

The two-dimensional thermo-hydraulic behavior during the reflood phase has been investigated using Slab Core Test Facility (SCTF)[1][2] which has a full radius slab section of a PWR. It has been revealed from the SCTF test results that the horizontal distribution of water head in the core was flat under various power profiles. However, the steep radial power profile gave the higher heat transfer in the higher power bundles under the same total core heating power[3]. The cross flow inside the core is considered to be the reason of the flow redistribution and the heat transfer enhancement in the higher power bundles. It has also been found in the SCTF test results that the collapsed water level in the upper plenum was higher toward the hot leg side and the nonuniform water accumulation in the upper plenum induced a nonuniform pressure distribution in the core[4]. The quench in the upper half of the core was delayed in the outer bundles probably due to the cross flow caused by the horizontal pressure gradient. Therefore, the quantitative evaluation of two-dimensional flow is important for the study of two-dimensional reflood phenomena.

Based on the single-phase air slanting flow experiment by Osakabe and Adachi[5], the flow-directional pressure loss in the rod bundle can be divided into two directions, parallel and normal to the rods, as in the case of COBRA-IV code[7]. Since the cross flow velocity has not been measured directly in the SCTF tests, the cross flow mass velocity has been estimated based on a homogeneous model using a cross flow resistance as well as measured horizontal differention pressures and void fractions[6]. The cross flow resistance in this calculating has been tentatively assumed to be 0.5 in accordance with COBRA-IV code model[7], which is a value for a water cross flow normal to a rod bundle in the absence of an axial flow component.

Weisman[8] developed a lateral momentum balance method for a single-phase cross flow in the presence of an axial flow component and presented a correlation which gives the cross flow resistance

coefficient as a function of the ratio of lateral velocity to axial velocity. However, the cross flow resistance under two-phase condition is considered to be affected by the presence of vapor phase. Osakabe and Adachi[9] carried out a two-phase air-water experiment in which a two-phase mixture slantingly attacked a rod bundle. In their test, however, the air and water was separated in the test vessel and the two-phase flow characteristics under the reflood phase could not be well simulated.

In the present study, a cross flow experiment is carried out in an air-water two-phase flow in a bundle geometry. A water cross flow is overlapped with the two-phase up-flow. Horizontal and vertical differential pressures are measured in this test. The cross flow resistance is obtained by assuming that only water phase can flow across the rod bundle with a specified velocity. By investigating the relation between the cross flow resistance and various flow parameters such as the vertical and horizontal water velocities, the vertical vapor velocity, the void fraction and the water viscosity, a correlation of cross flow resistance is derived as a function of void fraction and cross flow velocity. The effect of cross flow attack angle against the bundle lattice is also investigated because the fluid in the core can flow at any direction in an actual PWR.

2. TEST FACILITY

2.1 Test Facility

A schematic diagram of the cross flow test facility is shown in Fig. 2-1. Figure 2-2 shows the test section.

The rod bundle is arranged in 6×16 square array with the pitch of 14.3 mm. The rods are made of acrylic resin. The outer diameter of each rod is 10.7 mm and the length of the rod bundle is 1.0 m. The top and bottom ends of the rod bundle are fixed with spacers. Two additional grid spacers are installed in the middle elevations of the rod bundle, preventing the rods from bowing or moving. The configurations of the top, bottom, and intermediate spacers are shown in Fig. 2-3. The diameter and arrangement pitch of the rod bundle and the configuration of the intermediate spacers are based on those for a 15×15 fuel rod bundle of a Westinghouse type PWR.

The rod bundle is 85.8 mm depth and 228.8 mm width. In order to observe the flow pattern in the test section, the front and back plates of the test section are made of transparent acrylic resin.

The air injected through the perforated nozzles is mixed with the water injected through the bottom nozzle and the air-water mixture vertically flows into the rod bundle. Cross flow water is injected through the horizontal nozzle attached on the side wall of the test section and the same amount of water is extracted through the nozzle on the opposite side as shown in Fig. 2-2. In order to establish a local water cross flow overlapped with the vertical air-water two-phase flow in the rod bundle, a variable slit is installed along the injection and extraction sides of the rod bundle. The slit window gap can be varied from 10 to 180 mm. The configuration of the variable slit is shown in Fig. 2-4. The gaps between the slit and acrylic plates are sealed with rubber plates.

In order to investigate the effect of cross flow attack angle on the cross flow resistance, two additional test sections with different arrangement are used. The rod arrangements of test sections A, B and C are shown in Fig. 2-5. The cross flow attack angles for test sections A, B and C are 90°, 60° and 45°, respectively.

2.2 Instrumentation

The measurement items in the present tests are: horizontal and vertical differential pressures, air injection rate, vertical and horizontal water injection rates, horizontal water extraction rate and water temperature. The air and water flow rates were measured with rotor meters. The differential pressures were measured with strain gauge type D.P. cells in the tests with the slit width of 60 and 120 mm. In the tests with the slit width of 30 mm, a carbon tetrachloride/water manometer was used for the horizontal pressure measurement. Figure 2-6 shows the location and the dimension of pressure taps on the back plate. The pressure taps were located at the center of gap between two rods. The measurement spans of horizontal and vertical differential pressures are 143 mm and 100 mm, respectively.

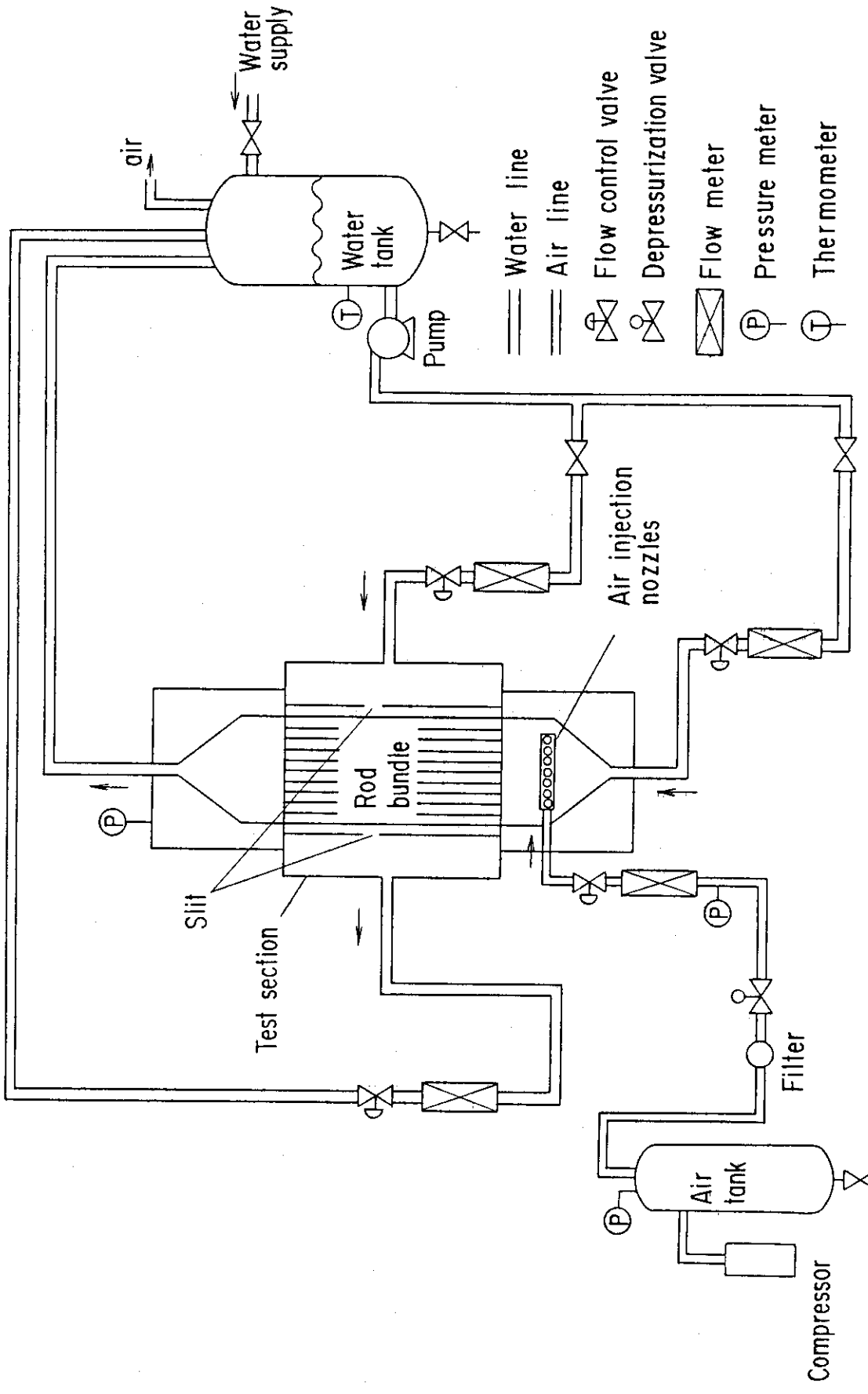

Fig. 2-1 Schematic diagram of cross flow test facility

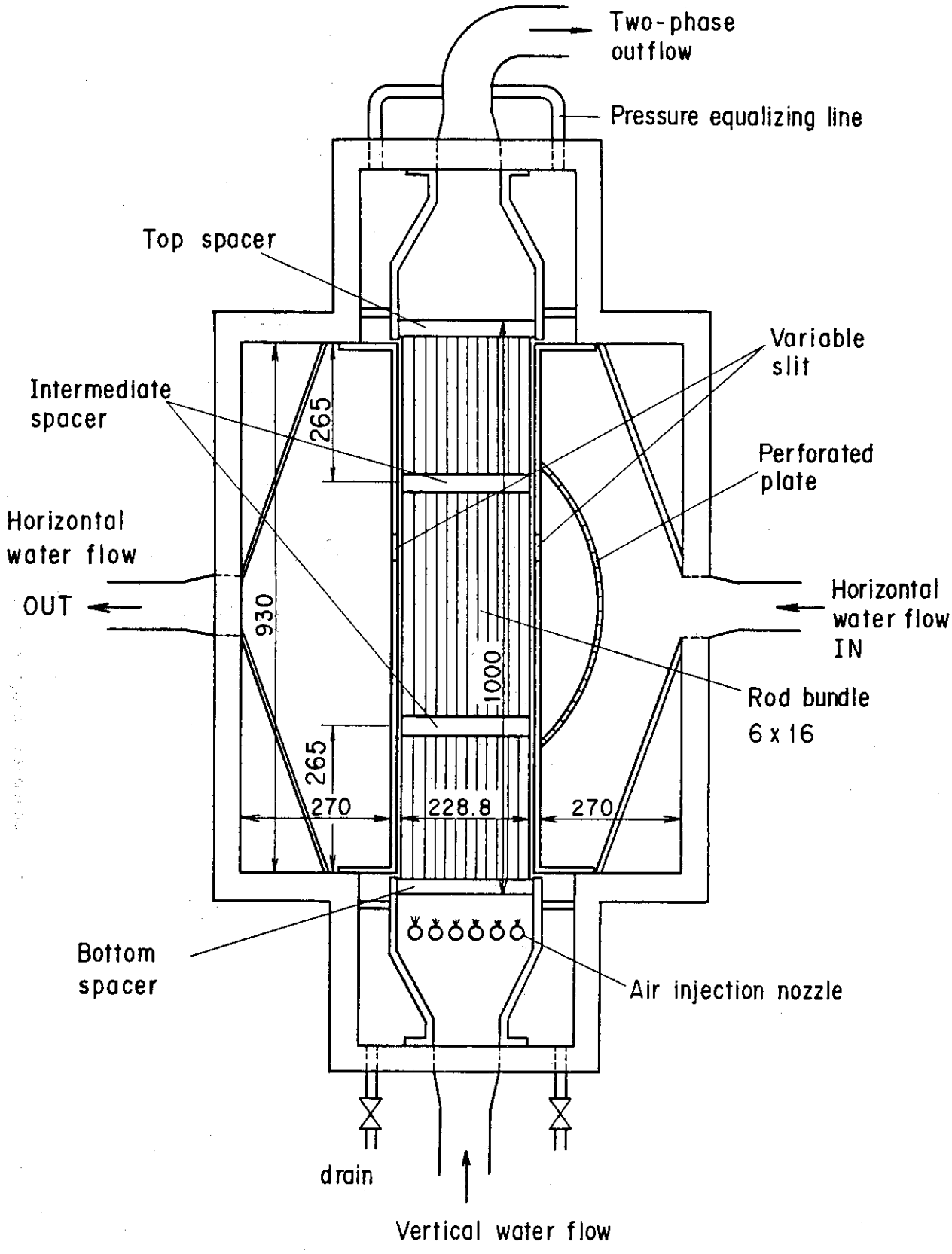

Fig. 2-2 Test section

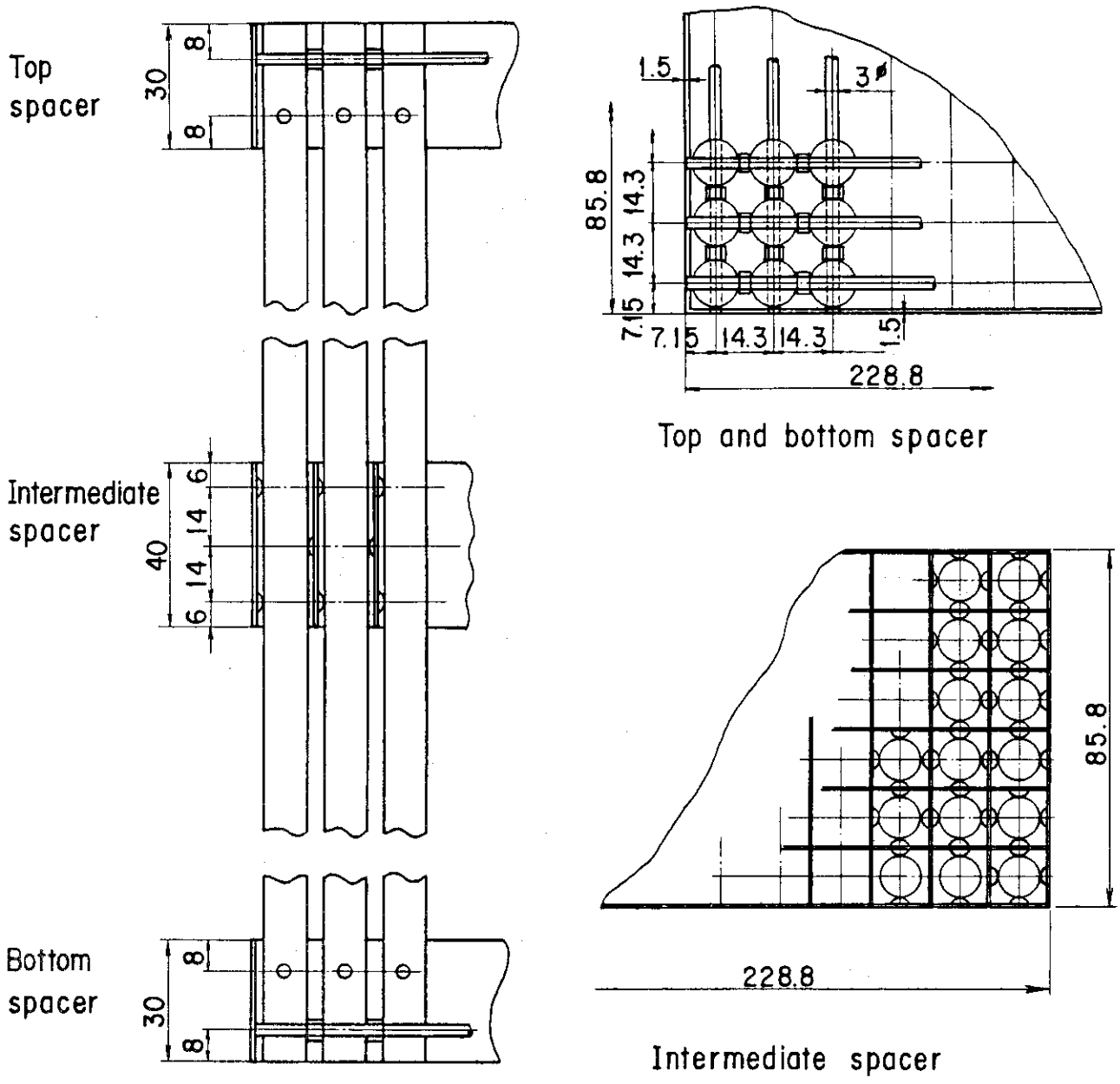

Fig. 2-3 Configurations of spacers

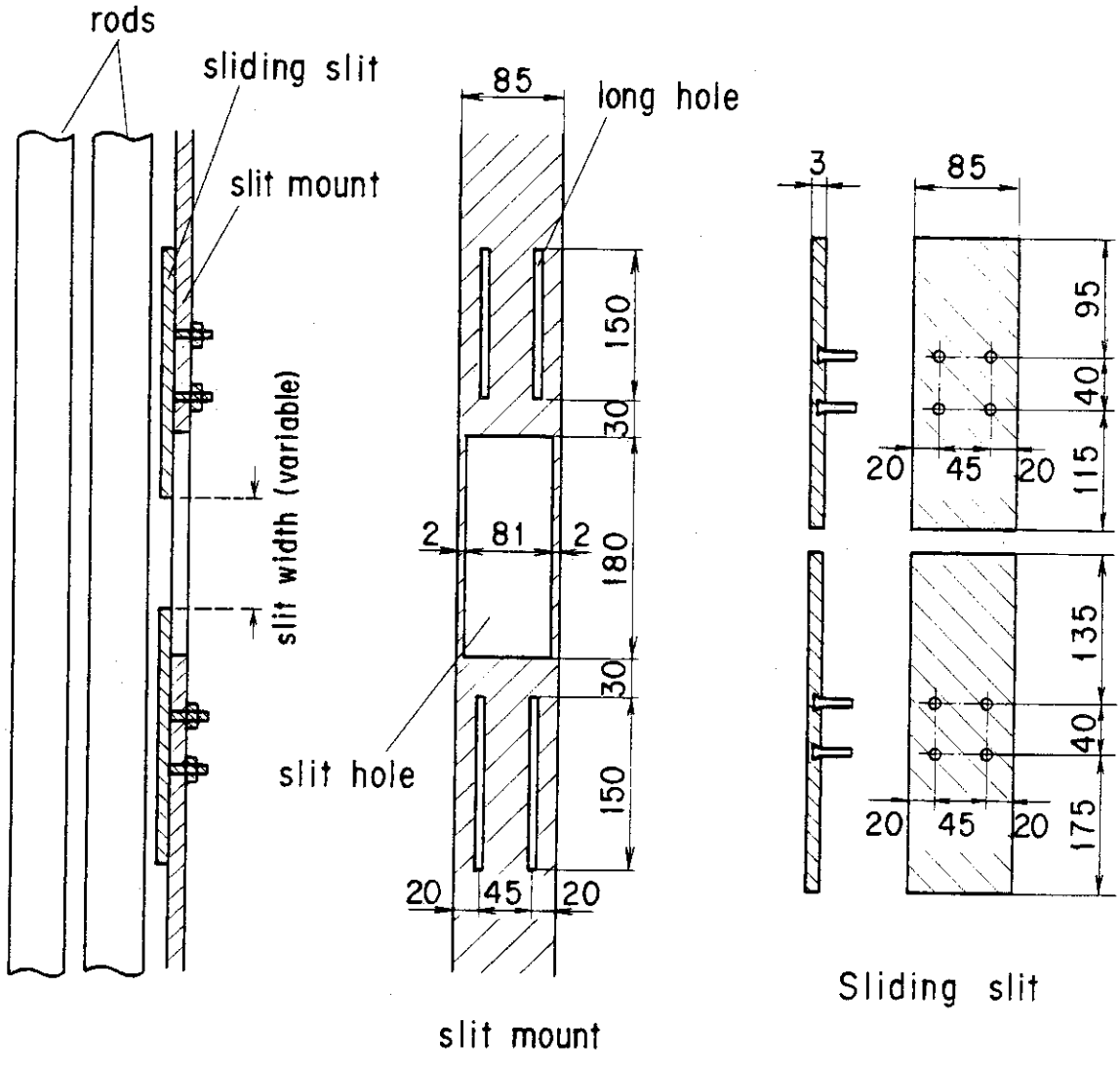

Fig. 2-4 Variable slit

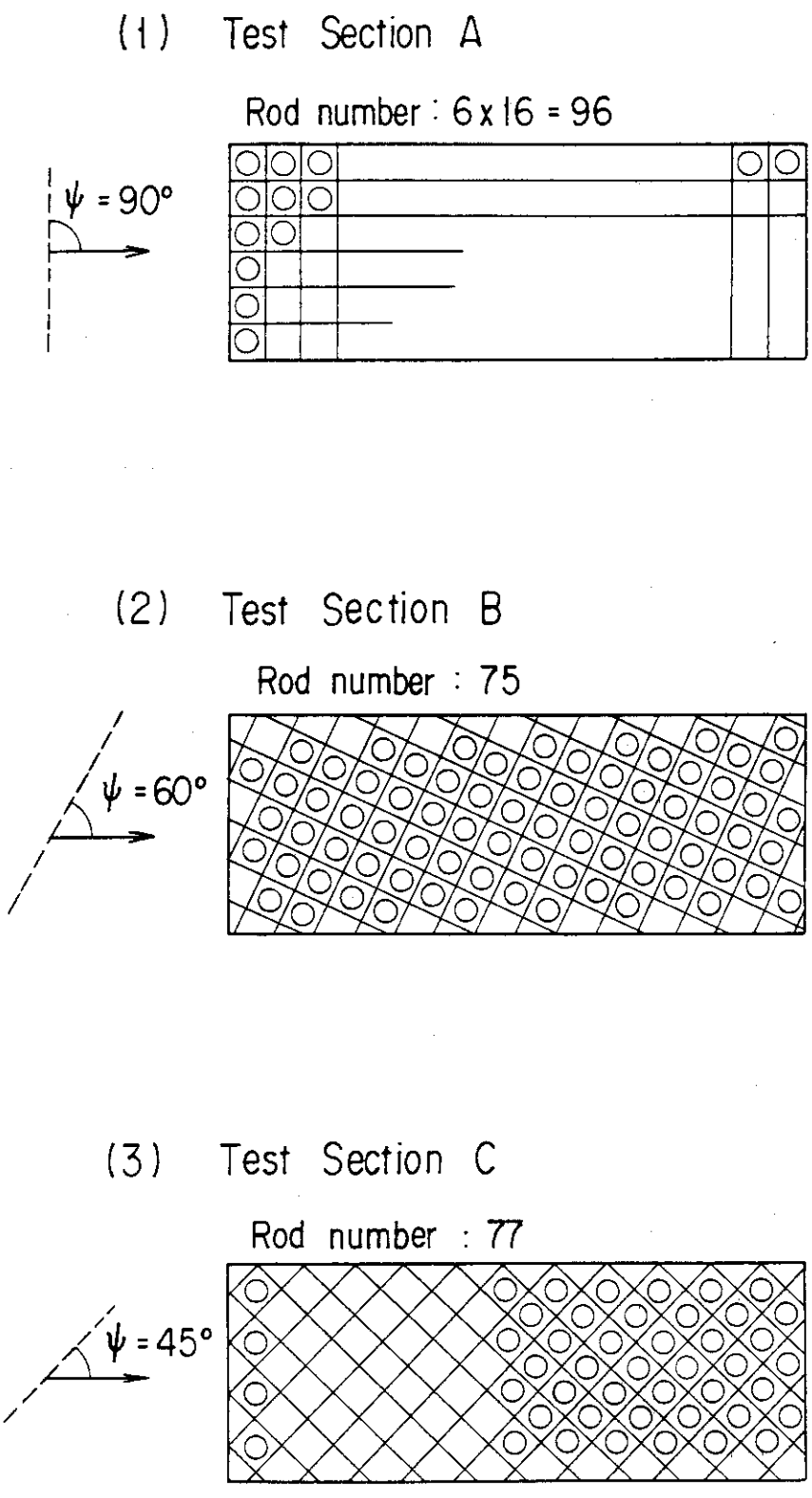

Fig. 2-5 Arrangement of rods in three test sections with different cross flow attack angles

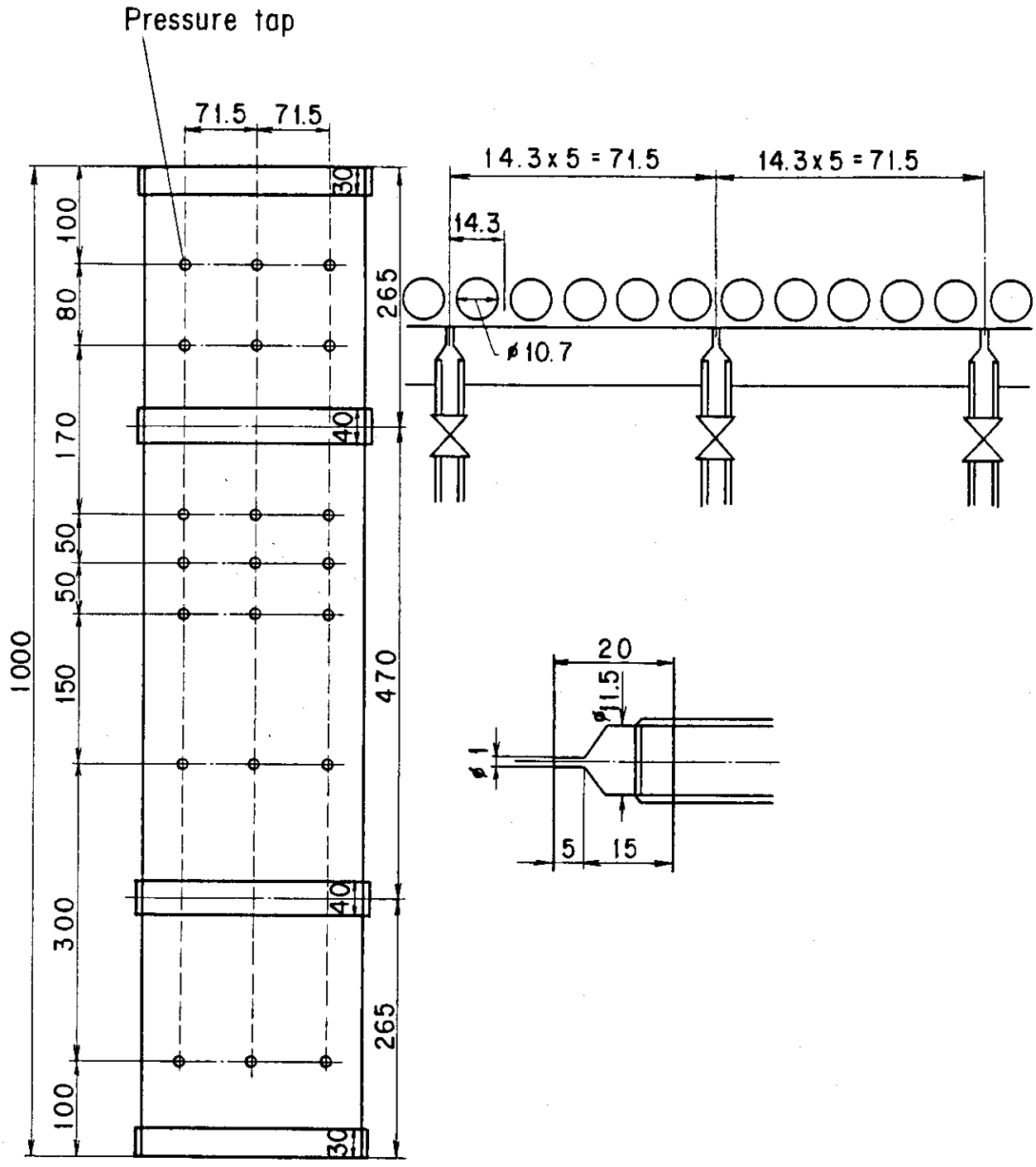

Fig. 2-6 Location and dimension of pressure tap

3. TEST RESULTS AND DISCUSSIONS

3.1 Two-Phase Flow Behavior in Rod Bundle

The two-phase flow pattern under the present test conditions was bubbly flow at low void fractions or slug flow at high void fractions. Examples of these two flow patterns are seen in Photos 3-1 and 3-2.

Since the water cross flow was added on the air-water vertical two-phase flow in the rod bundle, the concentration of air bubbles or slugs was higher in the cross flow outlet side and lower in the cross flow inlet side at the elevation of the slit width as seen in Photo 3-2. Figure 3-1 shows the horizontal distribution of void fractions measured at three horizontal locations. As shown in this figure, the void fraction is the highest at the cross flow outlet side and the lowest at the cross flow inlet side. However, it should be noted that the range of cross flow velocity in the present test was much higher than the cross flow velocity range expected in the reflood phase because the DP cell for the horizontal differential pressure could not measure the very low differential pressure caused by the low cross flow velocity. Since the void fraction at the center location well represents the average void fraction in the measurement range of the horizontal differential pressure as shown in Fig. 3-1, the void fraction at this location (ΔP_V^B in Fig. 3-1) is used for the cross flow resistance calculation in Section 3.2.

The two-phase flow pattern in the rod bundle was observed with a high speed video camera system with 200 frames per second. Based on this observation, the movement of air bubbles or slugs had a pulsation especially at higher air flow rates. Figure 3-2 shows some examples of horizontal and vertical differential pressure transients measured with DP cells. As shown in this figure, large oscillations of the differential pressures are observed especially at higher air flow rates. It was indicated by the slow motion pictures of the two-phase flow that the frequency of pulsation of flow was about 0.5 H_z and basically agreed with the frequency of the differential pressure oscillations.

The observations of two-phase flow behavior with the high speed video camera system show that most of the air bubbles or slugs tend to flow vertically along the rod bundle, indicating that the air cross flow rate was negligibly small in comparison to the vertical air flow rate. The same kind of two-phase flow behavior had been observed also in

the Osakabe and Adachi's experiment[5].

3.2 Cross Flow Resistance in Two-Phase Flow

3.2.1 Calculation Method

Since the observed air cross flow rate was negligibly small in comparison to the air vertical flow rate within the present experimental ranges, it can be assumed in the calculation of cross flow resistance that only water phase can flow transversally across the rods and all of the air bubbles or slugs flow only vertically. And the void fraction at the gap between rods is assumed to be 0.0. This assumption will be reviewed later. In addition, the horizontal differential pressure is assumed to be expressed with the same type equation as the single-phase water flow. The above-mentioned assumptions give the following relation between the horizontal differential pressure and the cross flow velocity through the gap between rods.

$$\Delta P_h = \frac{1}{2} C_D \rho_\ell V_{\ell h}^2 N_T \qquad (1)$$

The local water cross flow velocity, $V_{\ell h}$, in eq. (1) cannot be directly measured in the present test because of the expansion of a cross flow stream in the bundle. A cross flow expansion factor, f, is introduced so as to relate the local cross flow velocity, $V_{\ell h}$, to the cross flow velocity without flow expansion, $V_{\ell ho}$, by

$$f = \frac{V_{\ell ho}}{V_{\ell h}} . \qquad (2)$$

The cross flow expansion factor, f, is generally larger than the unity.

The horizontal differential pressure under single-phase water cross flow without flow expansion, ΔP_{ho}, can be related to the $V_{\ell ho}$ by

$$\Delta P_{ho} = \frac{1}{2} C_D^S \rho_\ell V_{\ell ho}^2 N_T \qquad (3)$$

Idel'chik[10] presented an equation of single phase cross flow resistance. The equation for a square rod array is given by

$$C_D^S = 1.52 \left(\frac{S}{D_{rod}} - 1 \right)^{-0.5} Re_h^{-0.2} \qquad (4)$$

where the cross flow water Reynolds number, Re_h, is defined as

$$Re_h = \frac{\rho_\ell V_{\ell h} D_{rod}}{\mu_\ell} \tag{5}$$

where the applicable range of Re_h in eq. (4) is $3 \times 10^3 < Re_h < 10^5$.

In the present experiment, the rod outer diameter is 10.7 mm, the square pitch is 14.3 mm, and the water temperature was about 20 °C. Then the cross flow resistance is written as

$$C_D^S = 0.4097\ V_{\ell h}^{-0.2} \tag{6}$$

Figure 3-3 shows the single-phase cross flow resistance calculated by eq. (6) against the cross flow velocity. As shown in Fig. 3-3, the cross flow resistance of 0.5 is a good approximation of the calculated cross flow resistance by eq. (6) within the present experimental range of cross flow velocities. The single-phase water cross flow resistance of 0.5 is also used in COBRA-IV code[7]. As also shown in Fig. 3-3, most of the estimated cross flow velocities in the present experiment are lower than the lower limit of the applicable range of eq. (6). Therefore, the single-phase cross flow resistance, C_D^S, is assumed to be 0.5 in eq. (3).

Since the cross flow stream can expand in the rod bundle, the local cross flow velocity, $V_{\ell h}$, is less than the $V_{\ell ho}$ and the measured horizontal differential pressure in the single-phase water cross flow experiment is given by

$$\Delta P_h = \frac{1}{2} C_D^S \rho_\ell V_{\ell h}^2 N_T \tag{7}$$

where $C_D^S = 0.5$ as in eq. (3)

From eqs. (3) and (7), the cross flow expansion factor, f, defined in eq. (2) can be obtained by

$$f = \left(\frac{\Delta P_{ho}}{\Delta P_h} \right)^{\frac{1}{2}}, \tag{8}$$

where the ΔP_{ho} can be calculated by eq. (3) and the ΔP_h can be measured with the DP cell.

By using the cross flow expansion factor, the cross flow resistance in eq. (1) can be obtained by

$$C_D = \frac{2\ f^2\ \Delta P_h}{\rho_\ell\ V^2_{\ell ho}\ N_T} \tag{9}$$

As mentioned before, eq. (1) is based on the assumption that no air phase exists at the gap between rods. However, some amount of air bubbles were observed to flow across the rods though the air cross flow rate was much less than the vertical air flow rate. In order to examine the effect of air phase at the gap between rods on the cross flow resistance, homogeneous flow is assumed as another limiting case. Thus the horizontal differential pressure is written as

$$\Delta P_h = \frac{1}{2}\ C_D^m\ \rho_m\ V^2_{mh}\ N_T \tag{10}$$

where $$\rho_m = \alpha\ \rho_g + (1-\alpha)\rho_\ell \tag{11}$$

Since ρ_g is much less than ρ_ℓ and α is less than 0.34 in the present experiment, ρ_m is approximately equal to $(1-\alpha)\rho_\ell$. Also the V_{mh} in eq. (10) is related to the $V_{\ell h}$ in eq. (1) by

$$V_{mh} = \frac{V_{\ell h}}{1-\alpha}\ . \tag{12}$$

Then, the cross flow resistance in the homogeneous model, C_D^m, is expressed by

$$C_D^m = \frac{2\ \Delta P_h (1-\alpha)^2}{(1-\alpha)\rho_\ell\ V^2_{\ell h}\ N_T} = (1-\alpha)\ C_D \tag{13}$$

Figure 3-4 shows the comparison of the two cross flow resistances obtained from eq. (9) and eq. (13). The actual cross flow resistance is considered to be between these two values. Since the void fraction at the gap between rods is considered to be much less than the void fraction at the subchannel especially for the higher void fraction, the C_D given by eq. (9) is adopted for the cross flow resistance in the present study. The difference between these two extreams increases with the void fraction and the maximum difference in the present experiment is 66 % due to the maximum void fraction of 0.34.

3.2.2 Cross Flow Expansion Factor

The cross flow expansion factor was obtained by a single-phase water cross flow experiment under various vertical and horizontal water velocities using eq. (8). The test results are summarized in Table A-1 in the Appendix. Listed in Table A-1 are; water cross flow rate ($Q_{\ell h}$), water cross flow velocity without flow expansion ($V_{\ell ho}$), horizontal differential pressure calculated by eq. (3) (ΔP_{ho}), vertical water flow rate ($Q_{\ell v}$), vertical water velocity ($V_{\ell v}$), measured horizontal differential pressure (ΔP_h), cross flow expansion factor calculated by eq. (8) (f), and local water cross flow velocity calculated by eq. (2) ($V_{\ell h}$).

Figures 3-5 and 3-6 show the measured horizontal differential pressures and the calculated cross flow expansion factors, respectively, as a function of the water cross flow velocity without flow expansion with the vertical water velocity as a parameter. As shown in these figures, the cross flow expansion factor gradually increases with the cross flow velocity without flow expansion except over 1.5 m/s in the slit width of 60 mm, while the horizontal differential pressure is a strong function of the cross flow velocity. The higher vertical water velocity tends to give the higher horizontal differential pressure and the lower flow expansion factor. The flow expansion factor becomes lower as the slit width increases.

The cross flow expansion factor listed in Table A-1 were used to calculate the two-phase cross flow resistance by eq. (9) for the conditions of the same horizontal and vertical water velocities and the slit width as the single-phase flow experiment.

3.2.3 Cross Flow Resistance in Two-Phase Flow

The ranges of test conditions of the two-phase cross flow experiments are listed in Table 3-1. The test results are listed in Tables A-2 through A-4 in the Appendix for the tests with the slit width of 30, 60 and 120 mm, respectively. Listed in these tables are; cross flow rate ($Q_{\ell h}$), cross flow velocity without flow expansion ($V_{\ell ho}$), vertical water flow rate ($Q_{\ell v}$), vertical superficial water velocity ($V_{\ell v}$), cross flow expansion factor (f) obtained in Section 3.1, local cross flow velocity calculated by eq. (2) ($V_{\ell h}$), vertical air flow rate (Q_{gv}), vertical superficial air velocity (V_{gv}), horizontal differential pressure (ΔP_h), void fraction (α), and cross flow resistance given by

eq. (9) (C_D). Water temperature (T_ℓ), dynamic viscosity (μ_ℓ), and horizontal water Reynolds number obtained by eq. (5) (Re_h) are also listed in these tables for deriving a correlation as will be discussed in Section 3.3.

The void fraction was calculated from the measured vertical differential pressure by neglecting the effects of frictional and accelerational pressure drops.

The measurement locations of the horizontal and vertical differential pressures for each slit width are shown in Fig. 3-7.

The cross flow resistances are plotted against the void fractions in Figs. 3-8 through 3-19 for each slit width and cross flow rate with the vertical superficial water velocity and the local cross flow velocity as parameters. In the present ranges of test parameters, the cross flow resistance is much higher in the two-phase air-water flow than in the single-phase water flow.

As typically shown in Figs. 3-8, 3-11, 3-15 and 3-16, the cross flow resistance increases approximately in proportion to the void fraction up to a certain critical value and above that value the cross flow resistance decreases with the void fraction. The critical void fraction increases with the cross flow velocity and the vertical superficial water velocity. When the cross flow velocity is higher than about 0.13 m/s, the cross flow resistance increases monotonously with the void fraction and no critical void fraction is observed in the present test ranges. The occurrence of peak cross flow resistance at a certin critical void fraction in the lower horizontal or vertical water velocity is considered to be attributed to the flow patern transition from a bubbly flow to a slug flow. Based on the flow observation with high speed video system, a bubbly flow was observed at the lower void fraction and a slug flow was observed at the higher void fraction under the cross flow velocity of 0.091 m/s and the vertical superficial water velocity of 0.0248 m corresponding to the data in Fig. 3-16.

It is also indicated from Figs. 3-8 through 3-19 that the cross flow resistance decreases with the cross flow velocity below the critical void fraction while the cross flow resistance is not much affected by the vertical water velocity.

3.3 Correlation of Cross Flow Resistance in Two-Phase Flow

Since the cross flow resistance increases with the void fraction and decreases with the cross flow velocity below the critical void fraction as mentioned in section 3.2, the cross flow resistance is considered to be represented by the following correlation;

$$C_D = C_1 \alpha^n Re_h^{-m} \quad . \tag{14}$$

where C_1, n and m are constant.

The horizontal water Reynolds number, Re_h, is given by eq. (5).

It is indicated from Figs. 3-8 through 3-19 that most of the cross flow resistances are approximately in proportion to the void fraction below the critical void fraction. Therefore, the n in eq. (14) is tentatively assumed to be 1.0.

In order to find the value of m in eq. (14), C_D/α is plotted against Re_h in Fig. 3-20 for the two slit width cases. It is indicated from Fig. 3-20 that the C_D/α can be fitted by the following equation;

$$C_D = 1.51 \times 10^5 \alpha Re_h^{-1.2} \quad . \tag{15}$$

As mentioned before, eq. (15) cannot represent the data point at the higher void fraction above the critical void fraction. The data points which were used to derive eq. (15) are marked with * in Table A-3 and A-4. The applicable ranges of eq. (15) are shown in Fig. 3-21 based on the test data ranges. It is found from Fig. 3-21 that the critical void fraction, α_{cr}, is represented by the following equation;

$$\alpha_{cr} = 0.0127 Re_h^{0.335} + 0.00448 \quad . \tag{16}$$

It should be also noted that eq. (15) cannot represent the effect of S/D_{rod} which is considered in the single-phase cross flow resistance equation (4) because the S/D_{rod} was not changed in the present experiment.

The calculated cross flow resistances using eq. (15) are compared with the test results in Figs. 3-11 through 3-19. Within the applicable ranges shown in Fig. 3-21, eq. (15) well agrees with the test results. By comparing eq. (15) with the single-phase cross flow

resistance equation (4), it is noted that the effect of the cross flow velocity on the cross flow resistance is much larger in the two-phase flow than in the single-phase flow.

It is also noted that the slit width has no effect on the relation between the C_D/α and the Re_h as shown in Fig. 3-20, suggesting that the estimation of the local cross flow velocity was not affected by the difference in the slit width between 60 and 120 mm.

3.4 Effect of Cross Flow Angle on Cross Flow Resistance

3.4.1 Test Conditions

In order to investigate the effect of cross flow attack angle against the bundle lattice on the cross flow resistance, the cross flow experiments were also performed by using Test Sections B and C in Fig. 2-5 with the attack angles of 60° and 45°, respectively. The ranges of test conditions for these experiments are listed in Table 3-2. The test results are listed in Tables A-5 and A-6 in the Appendix for the tests with attack angles of 60° and 45°, respectively. The slit width was 120 mm and the vertical water flow rate was fixed to 80 ℓ/min for these tests. It was revealed in Section 3.2.3 that the cross flow resistance was not much affected by the vertical water velocity.

3.4.2 Cross Flow Resistance for Rod Arrangement with Different Angle

The test results obtained from Test Sections B and C were compared with those from Test Section A to clarify the effect of cross flow attack angle on the cross flow resistance under two-phase flow condition. However, the cross flow resistance for a square rod array defined in eq. (9) cannot be used for the Test Sections B and C because the cross flow direction is not normal to the bundle lattice. In the present study, the cross flow resistance per unit length along the cross flow direction, C_D^o, was used. The definition is

$$C_D^o = \frac{\Delta P_h / L_h}{\frac{1}{2}\rho_\ell (V_{\ell h}^{in})^2} \qquad (17)$$

The unit of C_D^o is (m^{-1}) while the cross flow resistance defined in eq. (9) is dimensionless value. The cross flow expansion factor given by eq. (8) is not involved in eq. (17). That is, the cross flow expansion factor is considered to be the same for all of these three test sections.

3.4.3 Horizontal Differential Pressure in Single-Phase Water Cross Flow

Figure 3-22 shows the horizontal differential pressures in single-phase water cross flow vs. cross flow velocity at slit for Test Sections A, B and C. As shown in this figure, the horizontal differential pressure tends to decrease with decreasing the attack angle. The ratio of measured horizontal differential pressures between Test Sections C and A is approximately 0.7 in the present tests.

In order to evaluate the difference in the horizontal differential pressures between Test Sections A and C, the correlations of single phase cross flow resistances presented by Idel'chik[10] are used.

When the cross flow direction is normal to the square lattice, the cross flow resistance per single rod array is given by eq. (4). Therefore, the horizontal differential pressure in Test Section A can be expressed as

$$\Delta P_h^A = 1.52 \left(\frac{S}{D_{rod}} - 1 \right)^{-0.5} (Re_h^A)^{-0.2} N_A \cdot \frac{1}{2} \rho_\ell (V_{\ell h}^A)^2 \qquad (18)$$

On the other hand, the horizontal differential pressure in a bundle of staggered tubes is given by[10]

$$P_h^C = 0.44 \left(\frac{\sqrt{2}S - D_{rod}}{S - D_{rod}} + 1 \right)^2 (Re_h^C)^{-0.27} (N_c + 1) \cdot \frac{1}{2} \rho_\ell (V_{\ell h}^C)^2 \qquad (19)$$

By neglecting the difference in water temperatures in the single-phase cross flow experiments and substituting the relation of $V_{\ell h}^A = \sqrt{2}\, V_{\ell h}^C$, the ratio of $\Delta P_h^C / \Delta P_h^A$ is written by

$$\frac{\Delta P_h^C}{\Delta P_h^A} = 1.76 (Re_h^A)^{0.07} \qquad (20)$$

The relation between $(\Delta P_h^C / \Delta P_h^A)$ and (Re_h^A) based on eq. (20) is shown in Fig. 3-23. The present experimental range is also indicated in this figure. The ratio of horizontal differential pressure, $\Delta P_h^C / \Delta P_h^A$, is between 0.93 and 1.03 in the present experimental range, indicating that the horizontal differential pressure is not so much affected by the cross flow attack angle against the bundle lattice.

However, the measured horizontal differential pressure in Test Section C is approximately 30 % less than that in Test Section A as shown in Fig. 3-22. This discrepancy between the measured and calculated horizontal differential pressures in the single-phase cross flow is explained by the fact that there exists relatively large gap between the outer rods of Test Section C and the front and back plates and therefore the effective cross flow resistance is lower in Test Section C than in an actual staggered rod bundle.

3.4.4 Cross Flow Resistance in Two-Phase Flow

Figures 3-24 and 3-25 show the cross flow resistances defined by eq. (17) vs. void fractions in Test Sections A, B and C. The cross flow resistance tends to decrease with decreasing the attack angle especially at the higher void fraction and lower cross flow velocity. However, as discussed in Section 3.4.3, the large gap between the rod bundle and the shroud walls in Test Section C is considered to be the major reason of the lower cross flow resistance in Test Section C than in Test Section A. On the other hand, while the cross flow resistances are slightly smaller in Test Section B than in Test Section A, the difference in the cross flow resistances between Test Sections B and A is much less than that between Test Sections C and A because the gap between the outer rod and the flow shround walls is smaller in Test Section B than in Test Section C as shown in Fig. 2-5.

Therefore it is concluded that the effect of attack angle on the cross flow resistance is considered to be much less than 30 % below the critical void fraction, while the cross flow resistance tends to decrease slightly with decreasing the attack angle.

Table 3-1 Test conditions of two-phase cross flow experiments

	Symbol	Unit	Range
Slit width	H	(mm)	30, 60 120
Cross flow rate	$Q_{\ell h}$	(ℓ/min)	30 ~ 150
Cross flow velocity without flow expansion	$V_{\ell ho}$	(m/s)	0.224 ~ 2.99
Cross flow velocity*	$V_{\ell h}$	(m/s)	0.056 ~ 0.327
Vertical water flow rate	$Q_{\ell v}$	(ℓ/min)	15 ~ 150
Vertical superficial water velocity	$V_{\ell v}$	(m/s)	0.0248 ~ 0.248
Vertical air flow rate	Q_{gv}	(ℓ/min)	17.3 ~ 863
Vertical superficial air velocity	V_{gv}	(m/s)	0.0285 ~ 1.42
Void fraction	α		0 ~ 0.34
Horizontal water Reynolds number	Re_h		550 ~ 5640

* Cross flow velocity is calculated by eq. (2) using a cross flow expansion factor.

Table 3-2 Test conditions of two-phase cross flow experiments in Test Sections B and C

	Symbol	Unit	Range
Attack angle	ψ	(degree)	60,45
Slit width	H	(mm)	120
Cross flow rate	$Q_{\ell h}$	(ℓ/min)	30 ~ 100
Cross flow velocity at slit	$V_{\ell h}^{in}$	(m/s)	0.0485~0.162
Vertical water flow rate	$Q_{\ell v}$	(ℓ/min)	80
Vertical superficial water velocity	$V_{\ell v}$	(m/s)	0.104~0.121 m/s
Vertical air flow rate	Q_{gv}	(ℓ/min)	0 ~ 1290
Vertical superficial air velocity	V_{gv}	(m/s)	0 ~ 1.69
Void fraction	α		0 ~ 0.44

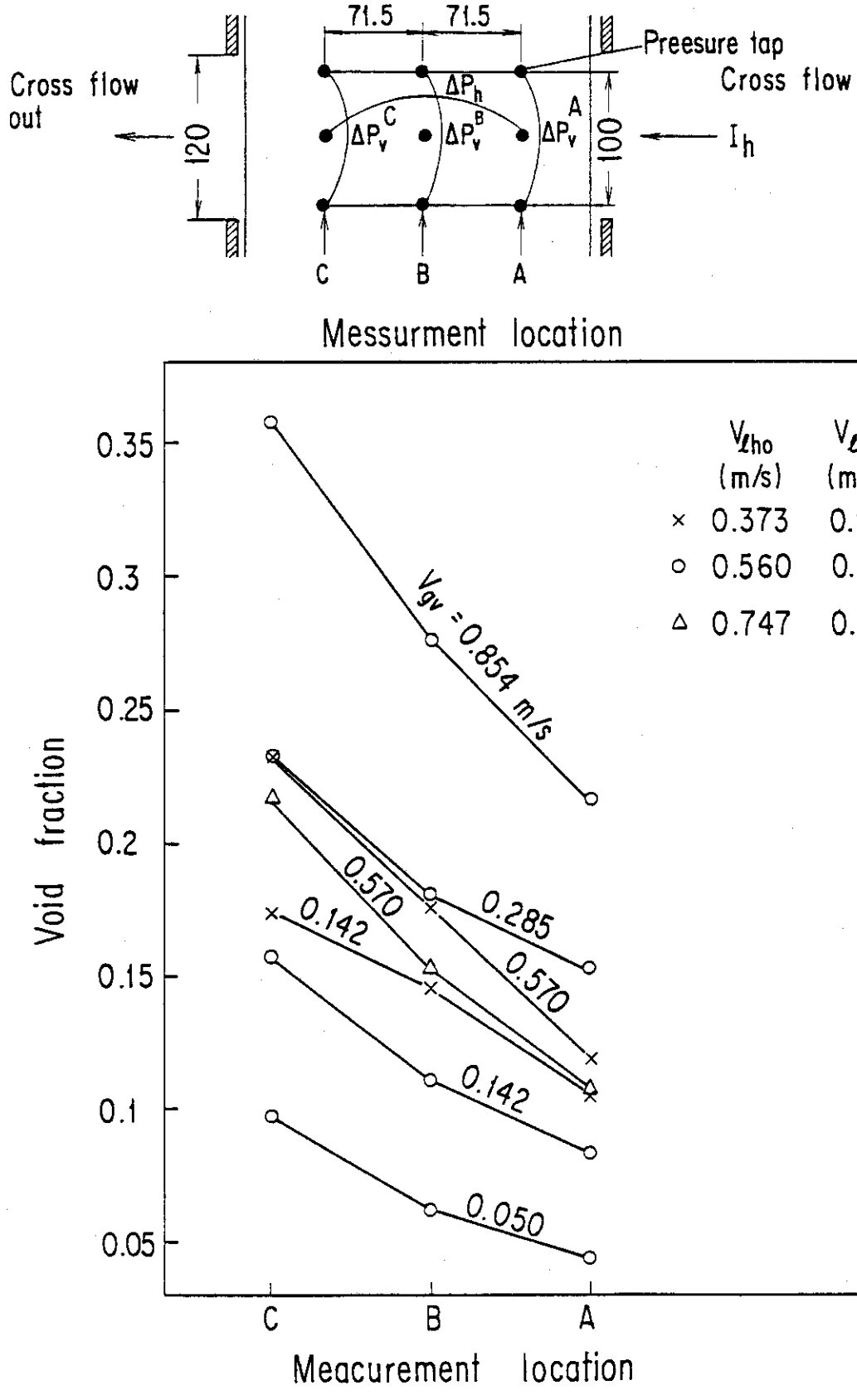

Fig. 3-1 Horizontal distribution of void fractions

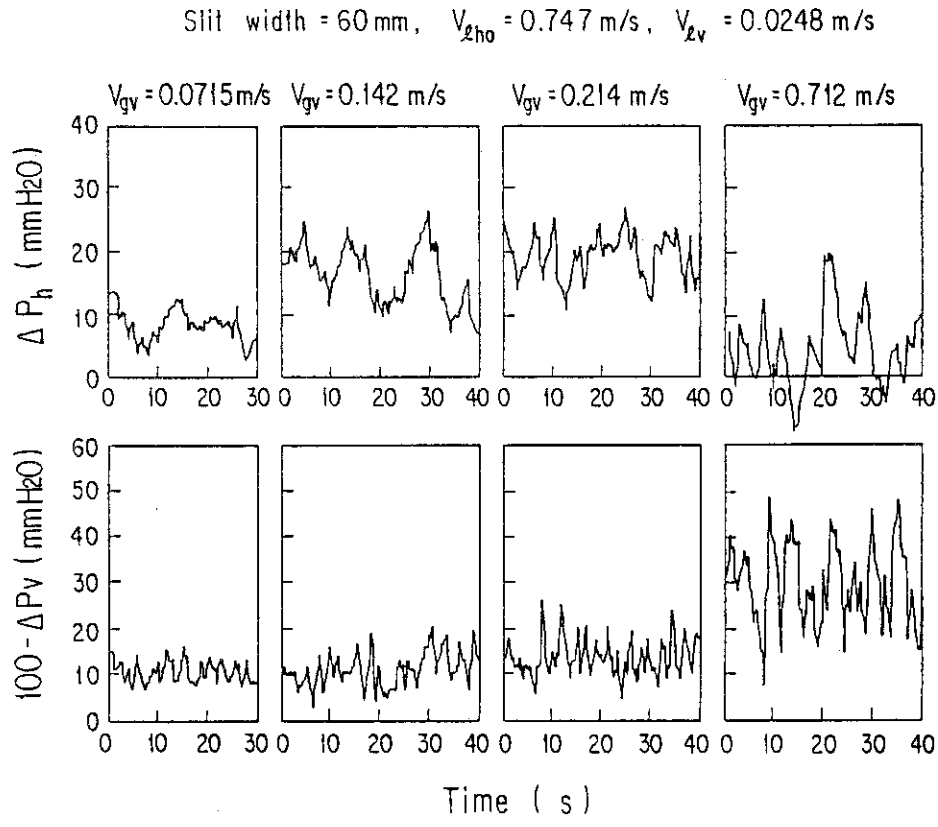

Fig. 3-2 Examples of horizontal and vertical differential pressure transients

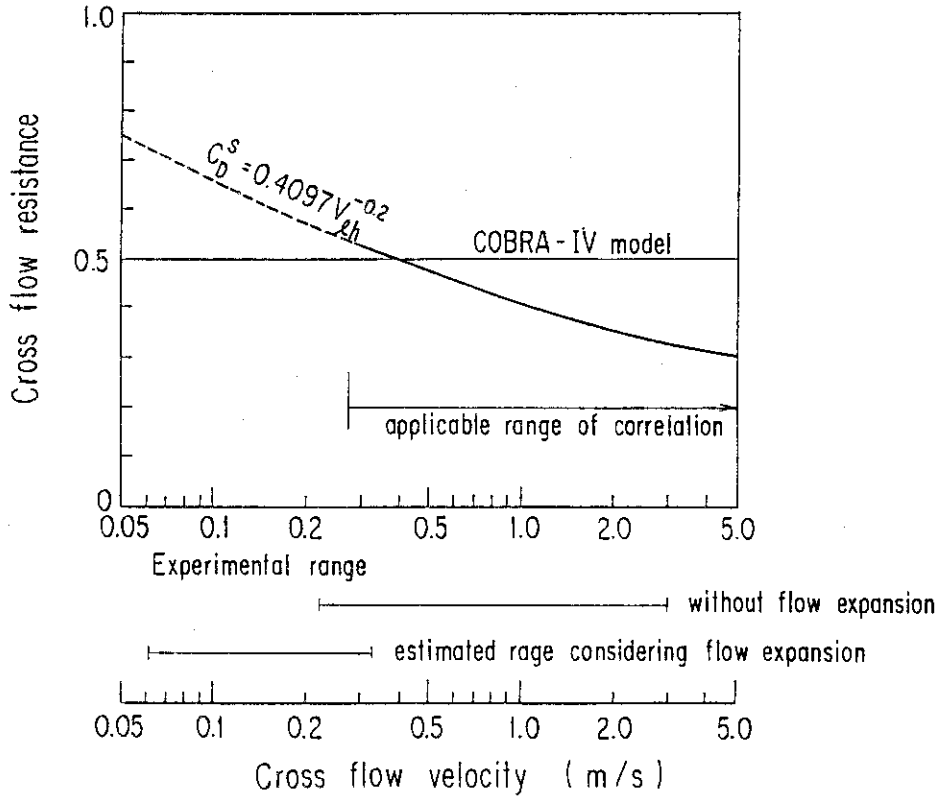

Fig. 3-3 Single-phase cross flow resistance vs. cross flow velocity

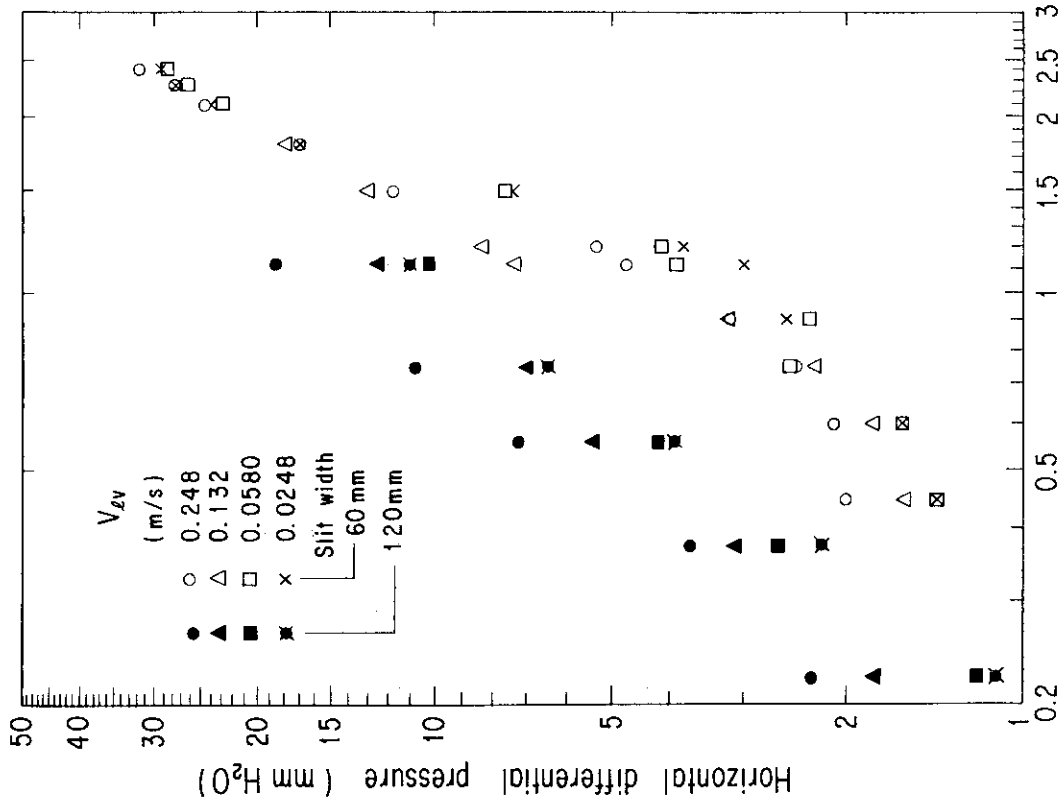

Fig. 3-5 Horizontal differential pressure vs. cross flow velocity without flow expansion in single-phase water flow

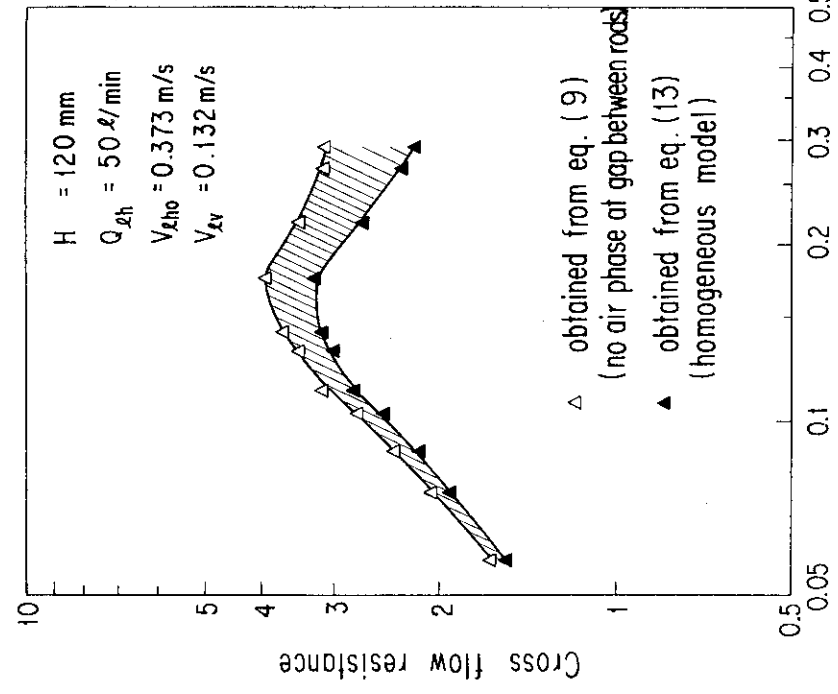

Fig. 3-4 Comparison of cross flow resistances obtained from two assumptions: no air phase at gap between rods and homogeneous two-phase mixture

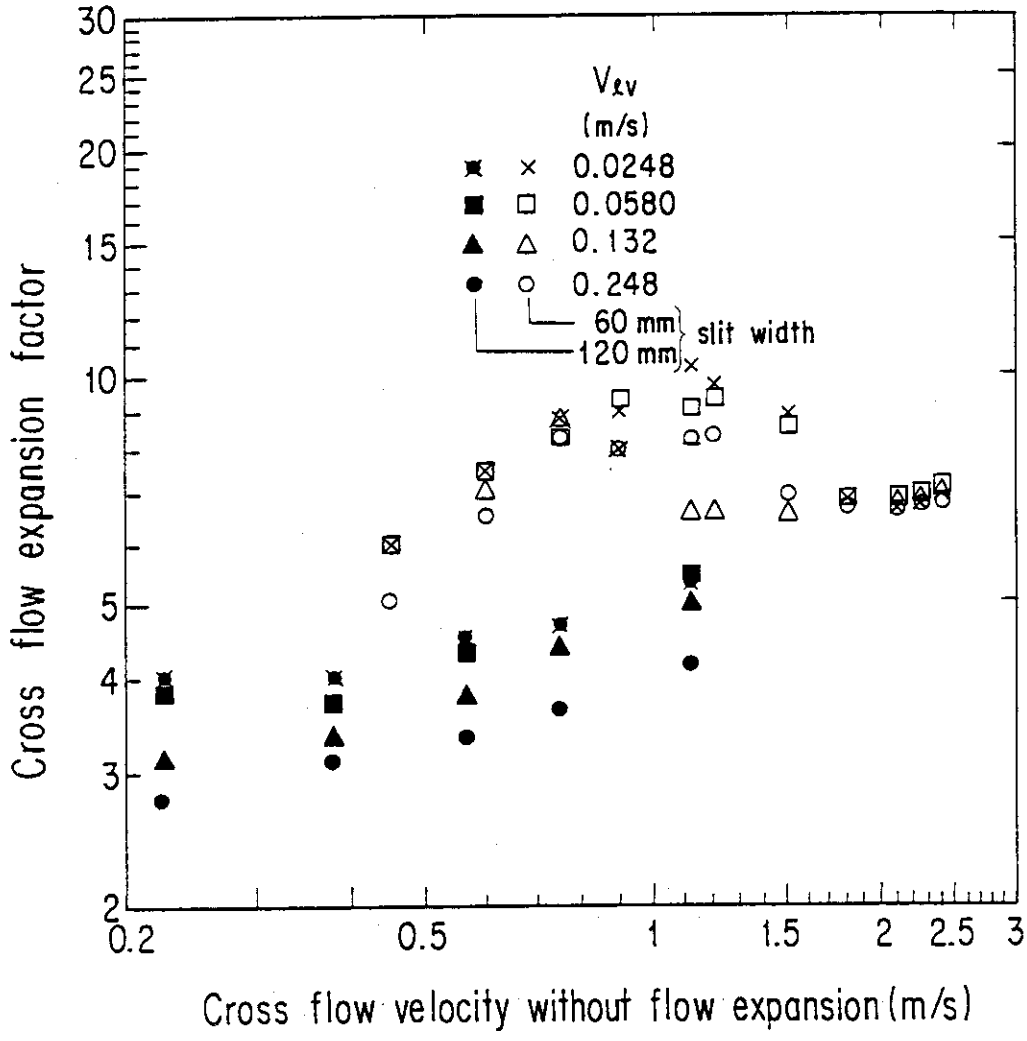

Fig. 3-6 Cross flow expansion factor vs. cross flow velocity without flow expansion in single-phase water flow

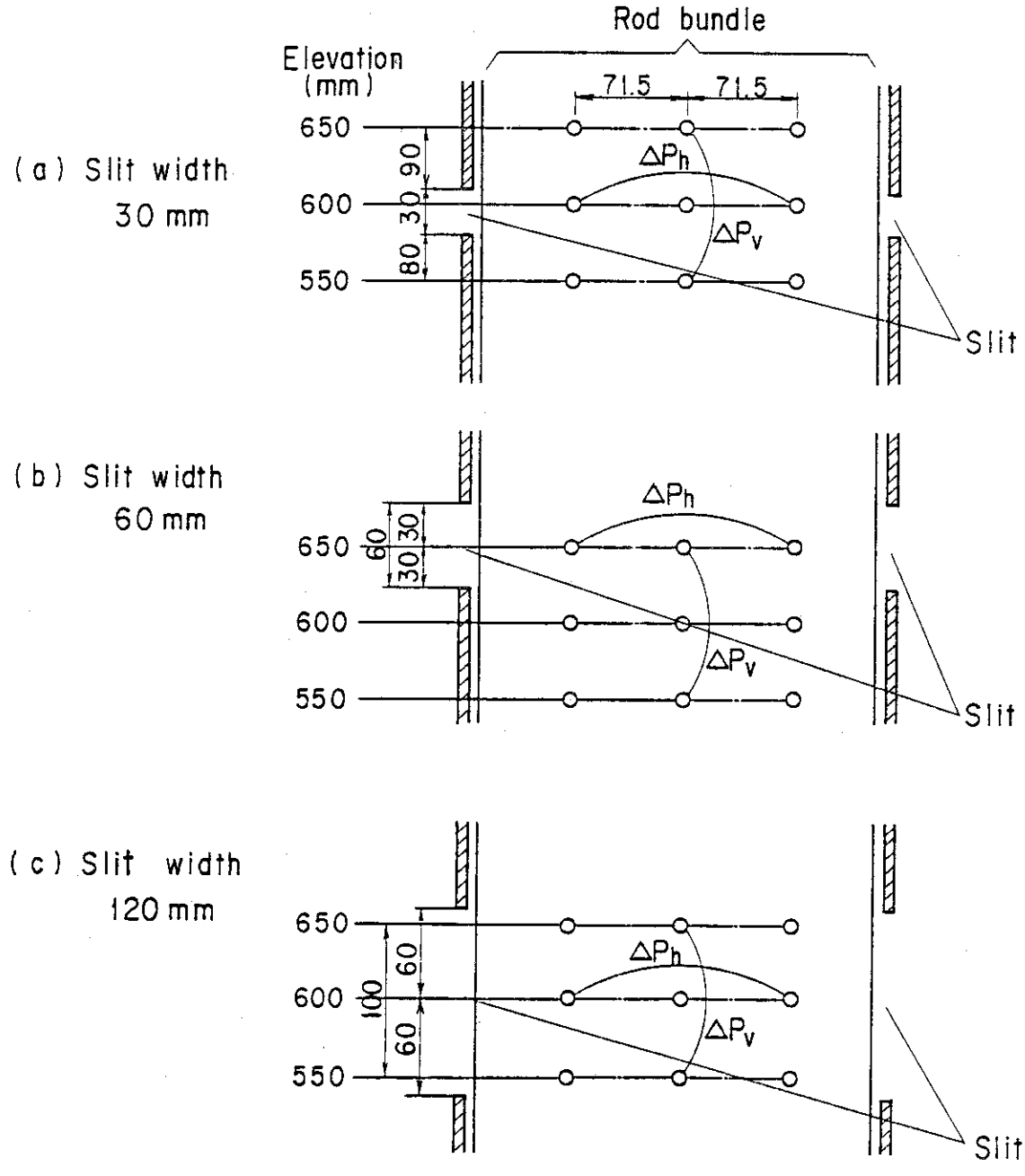

Fig. 3-7 Measurement locations of horizontal and vertical differential pressure

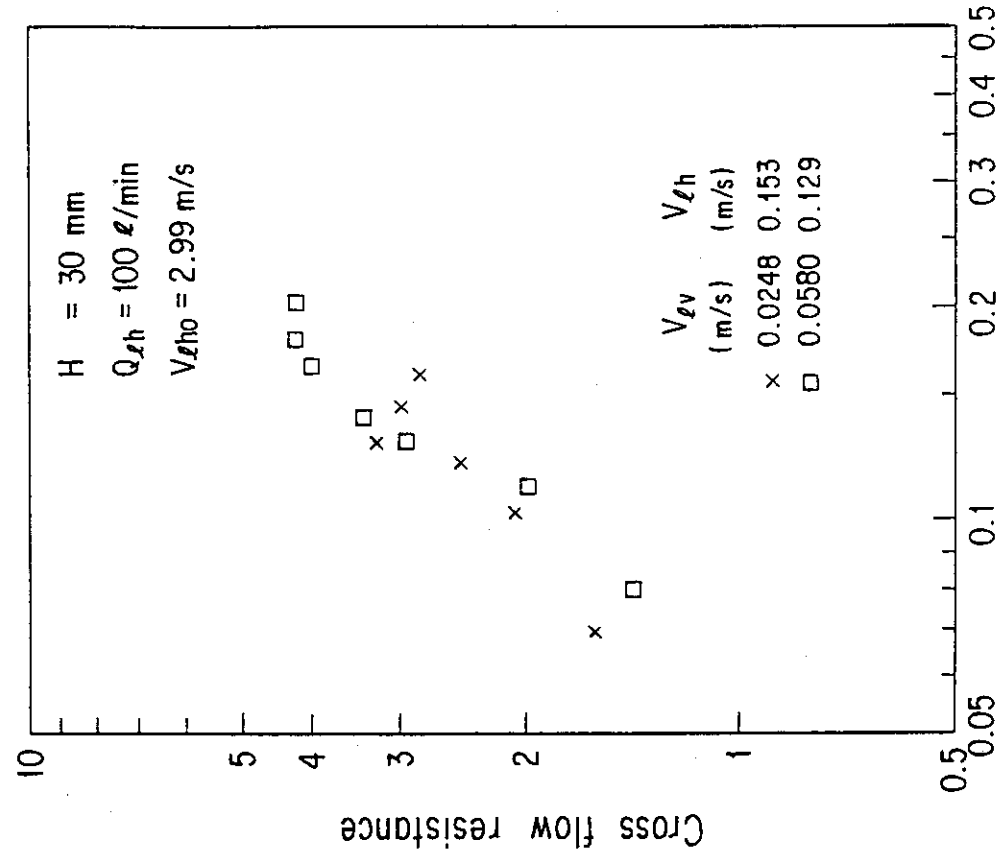

Fig. 3-9 Cross flow resistance vs. void fraction
(H = 30 mm, $Q_{\ell h}$ = 100 ℓ/min)

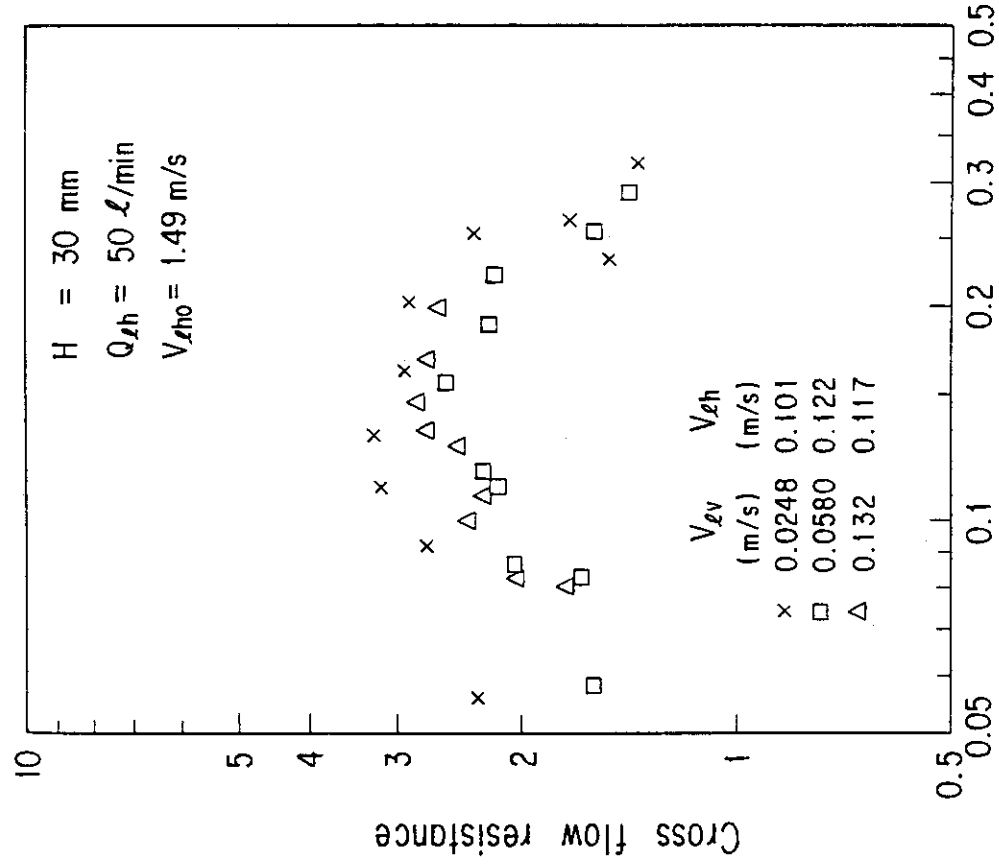

Fig. 3-8 Cross flow resistance vs. void fraction
(H = 30 mm, $Q_{\ell h}$ = 50 ℓ/min)

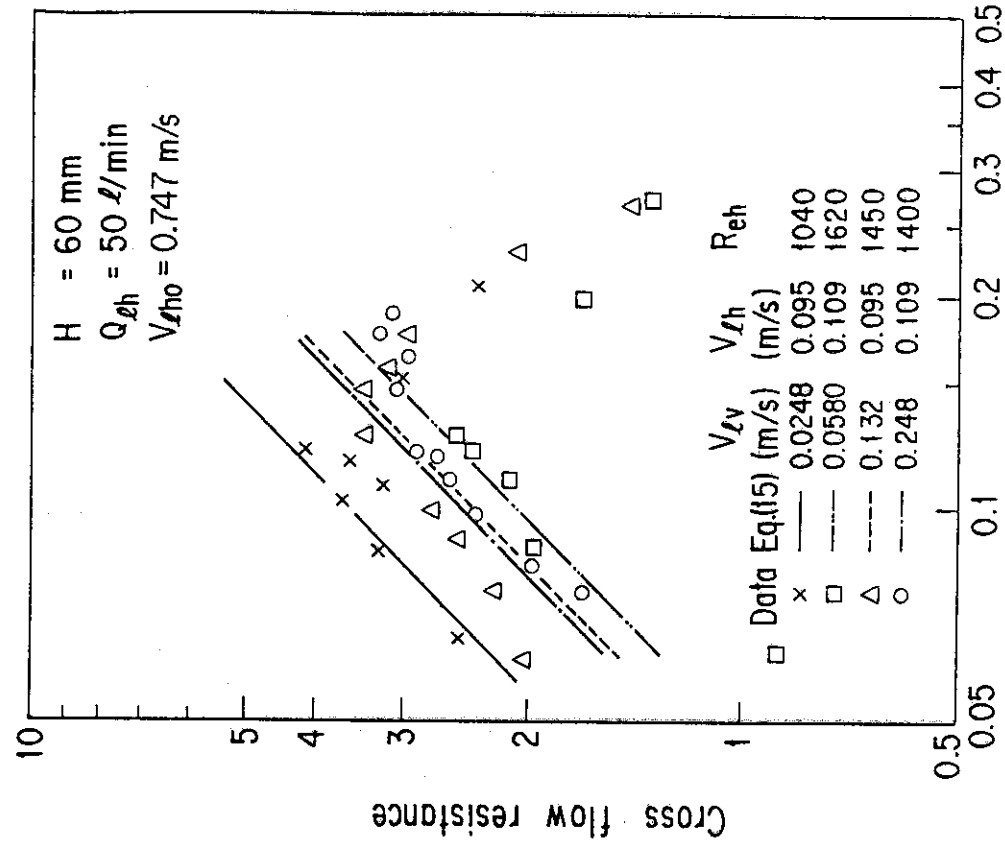

Fig. 3-11 Cross flow resistance vs. void fraction
(H = 60 mm, $Q_{\ell h}$ = 50 ℓ/min)

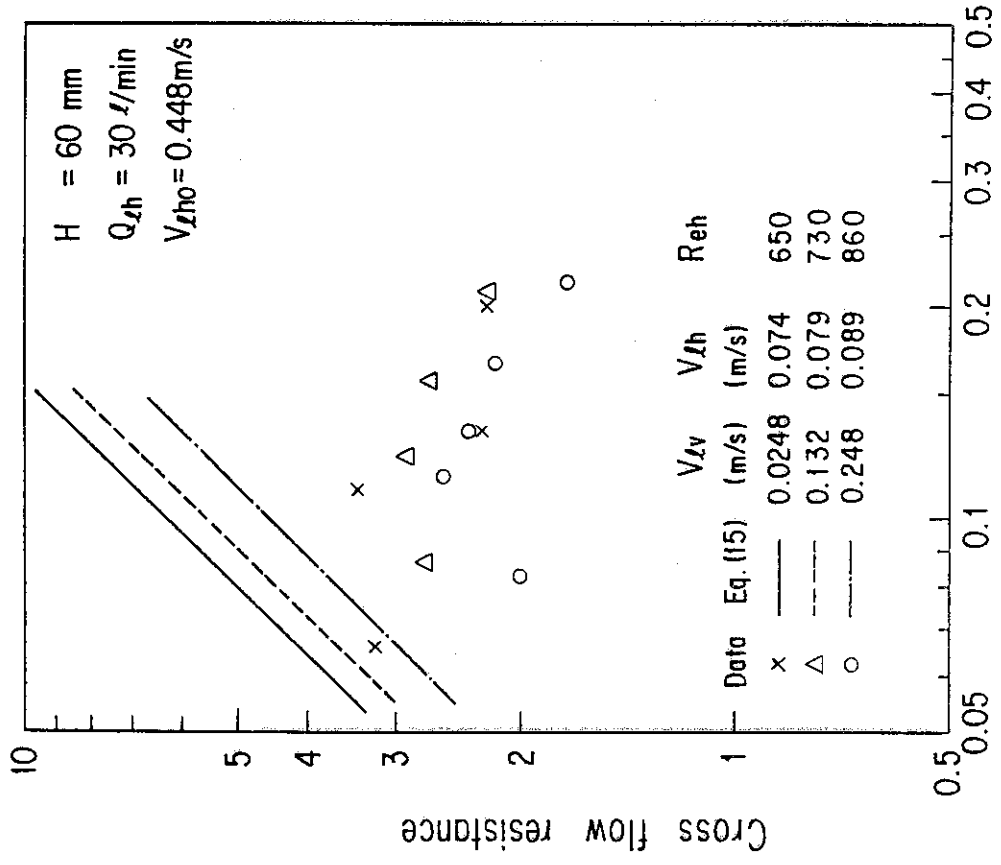

Fig. 3-10 Cross flow resistance vs. void fraction
(H = 60 mm, $Q_{\ell h}$ = 30 ℓ/min)

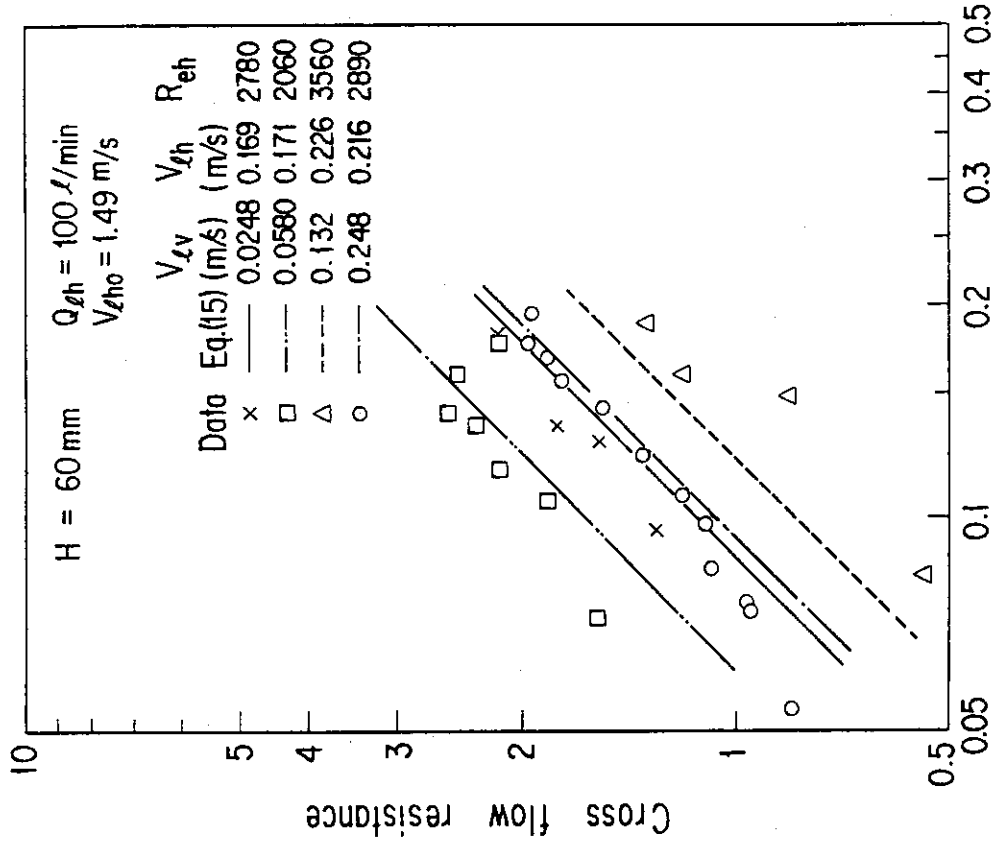

Fig. 3-13 Cross flow resistance vs. void fraction
(H = 60 mm, $Q_{\ell h}$ = 100 ℓ/min)

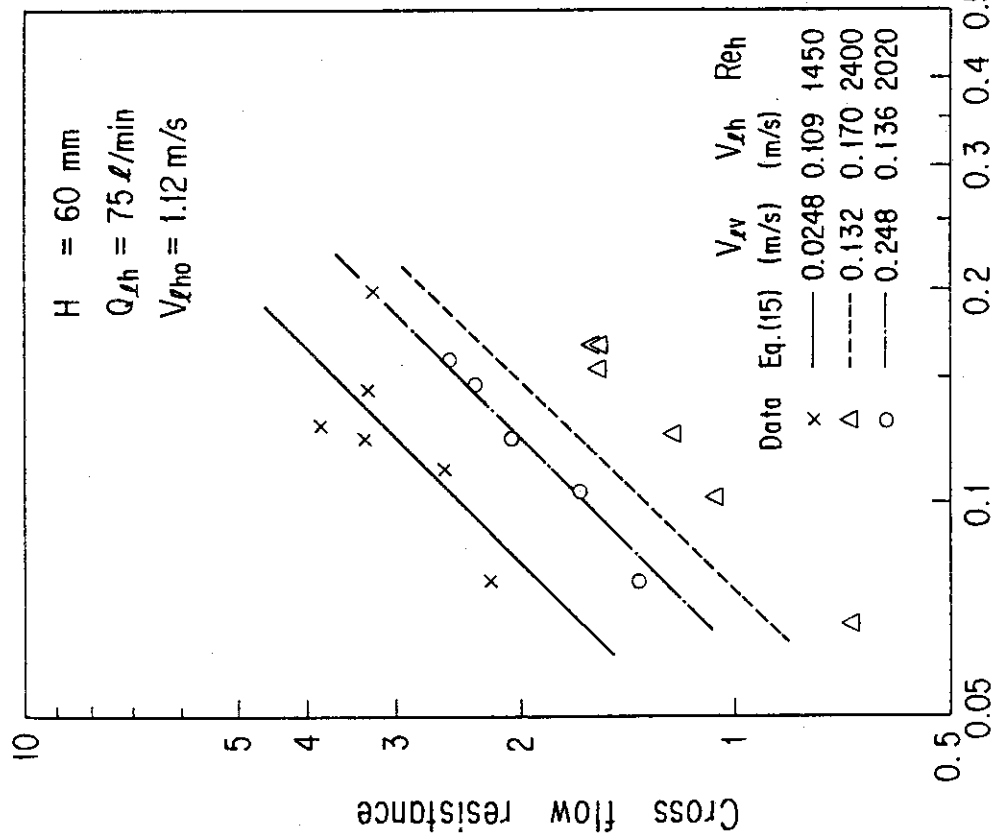

Fig. 3-12 Cross flow resistance vs. void fraction
(H = 60 mm, $Q_{\ell h}$ = 75 ℓ/min)

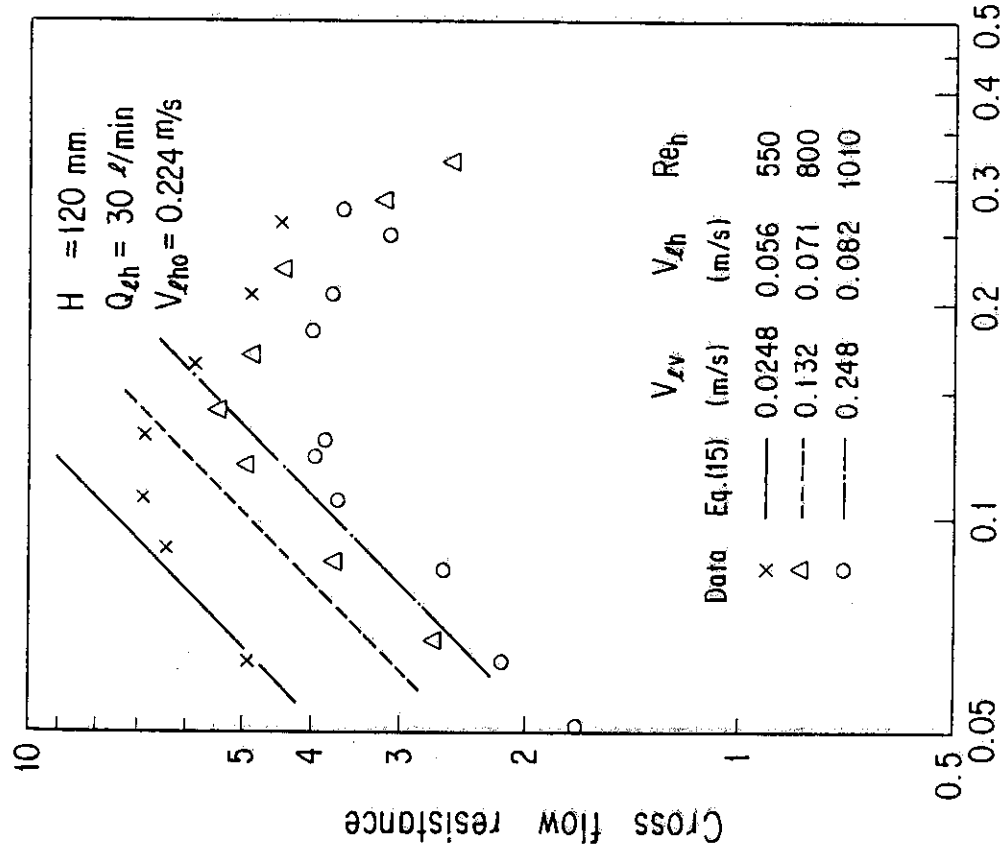

Fig. 3-15 Cross flow resistance vs. void fraction
(H = 120 mm, $Q_{\ell h}$ = 30 ℓ/min)

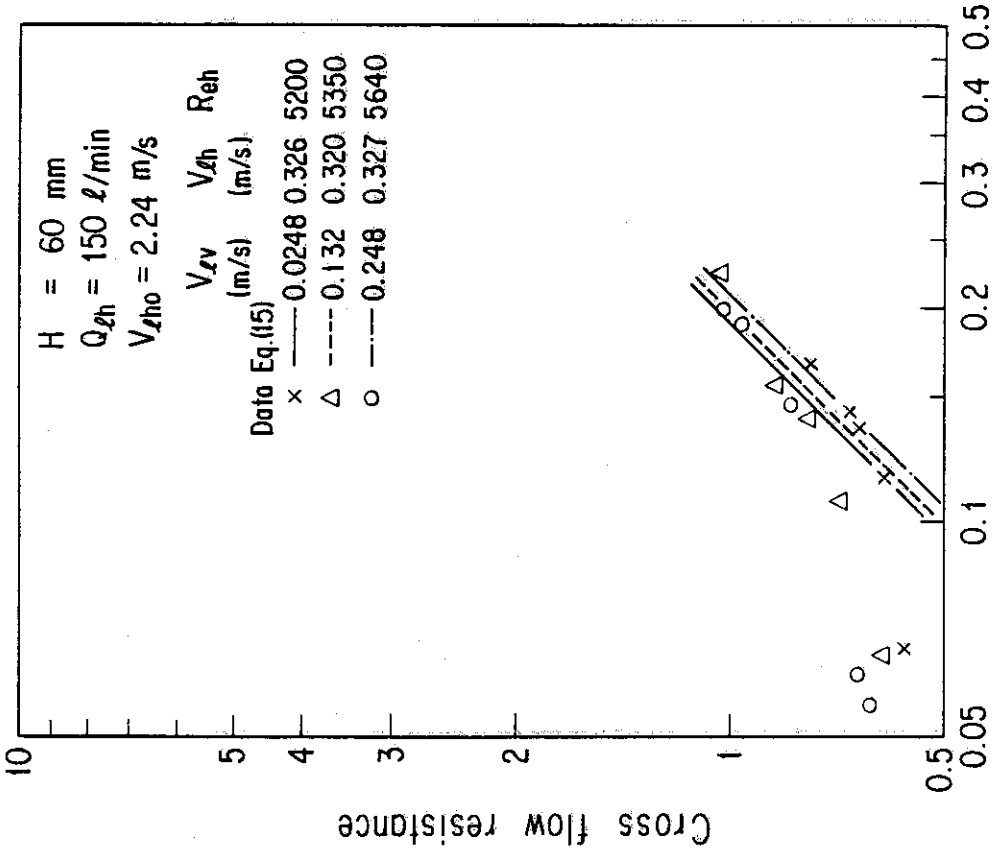

Fig. 3-14 Cross flow resistance vs. void fraction
(H = 60 mm, $Q_{\ell h}$ = 150 ℓ/min)

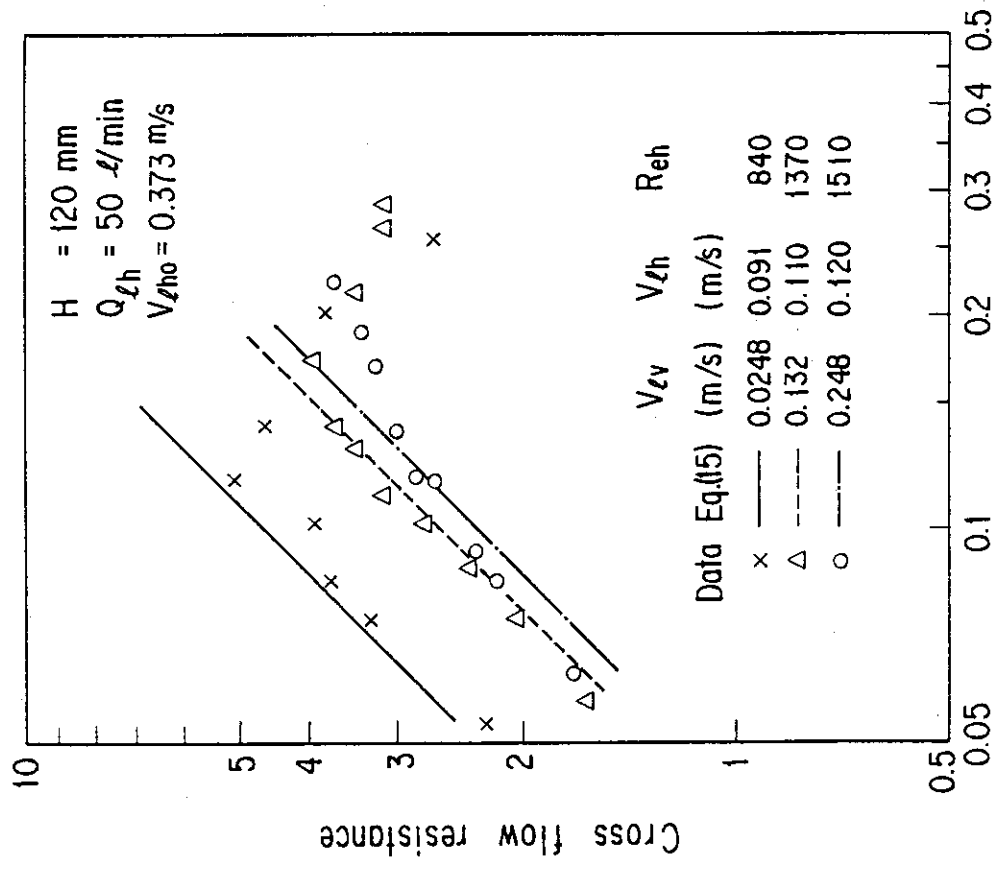

Fig. 3-16 Cross flow resistance vs. void fraction
(H = 120 mm, $Q_{\ell h}$ = 50 ℓ/min)

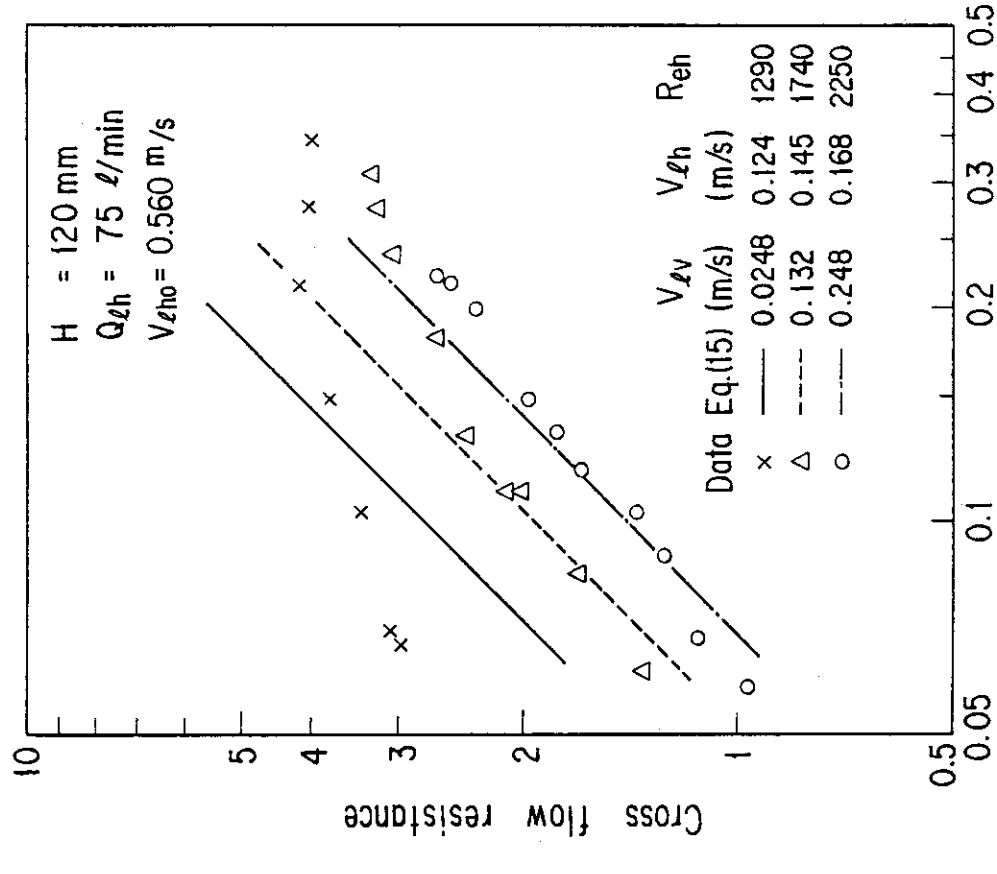

Fig. 3-17 Cross flow resistance vs. void fraction
(H = 120 mm, $Q_{\ell h}$ = 75 ℓ/min)

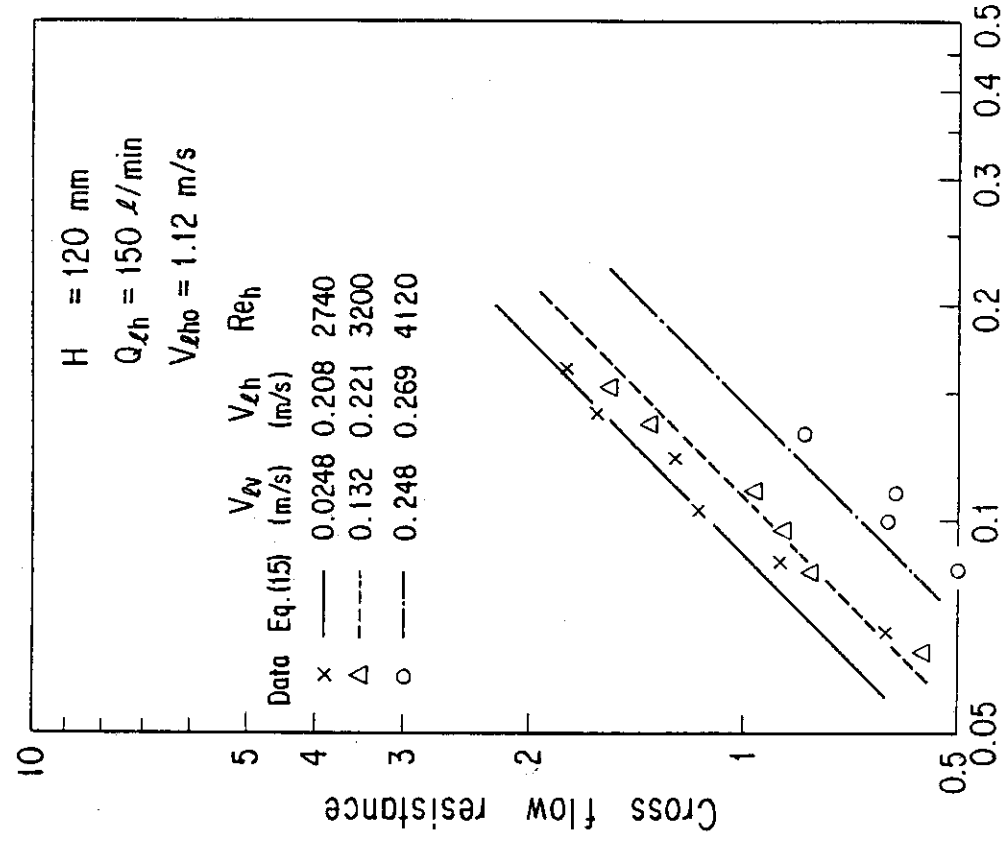

Fig. 3-19 Cross flow resistance vs. void fraction (H = 120 mm, $Q_{\ell h}$ = 150 ℓ/min)

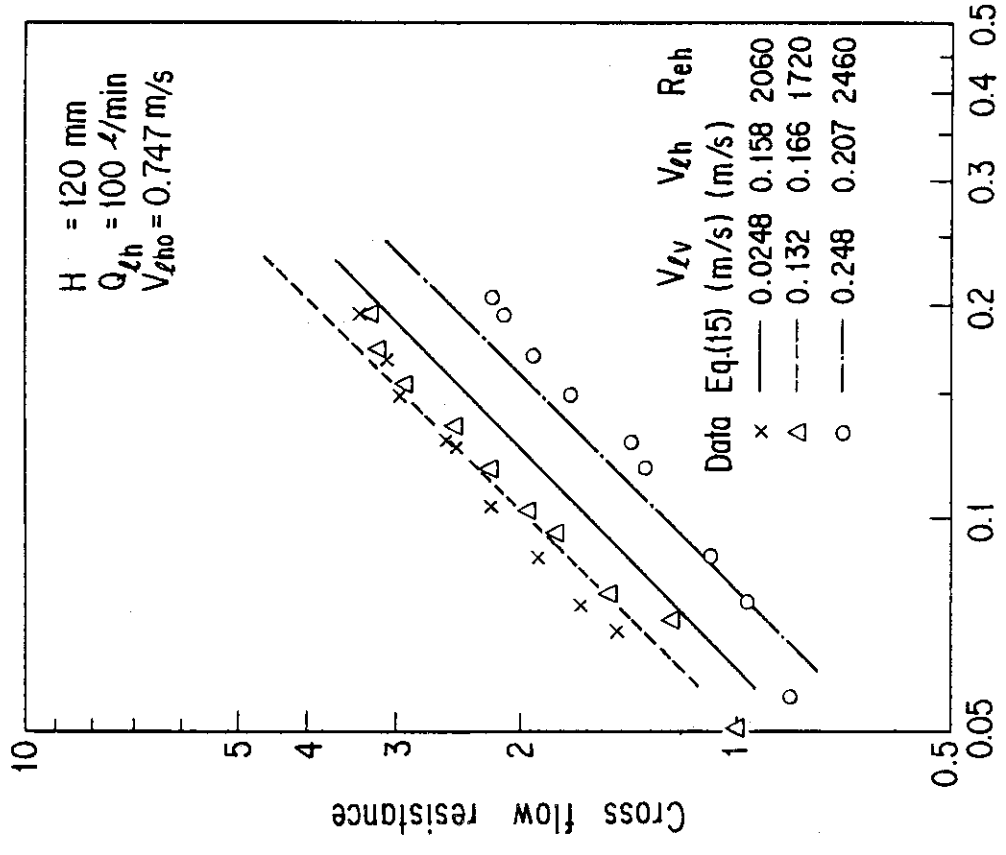

Fig. 3-18 Cross flow resistance vs. void fraction (H = 120 mm, $Q_{\ell h}$ = 100 ℓ/min)

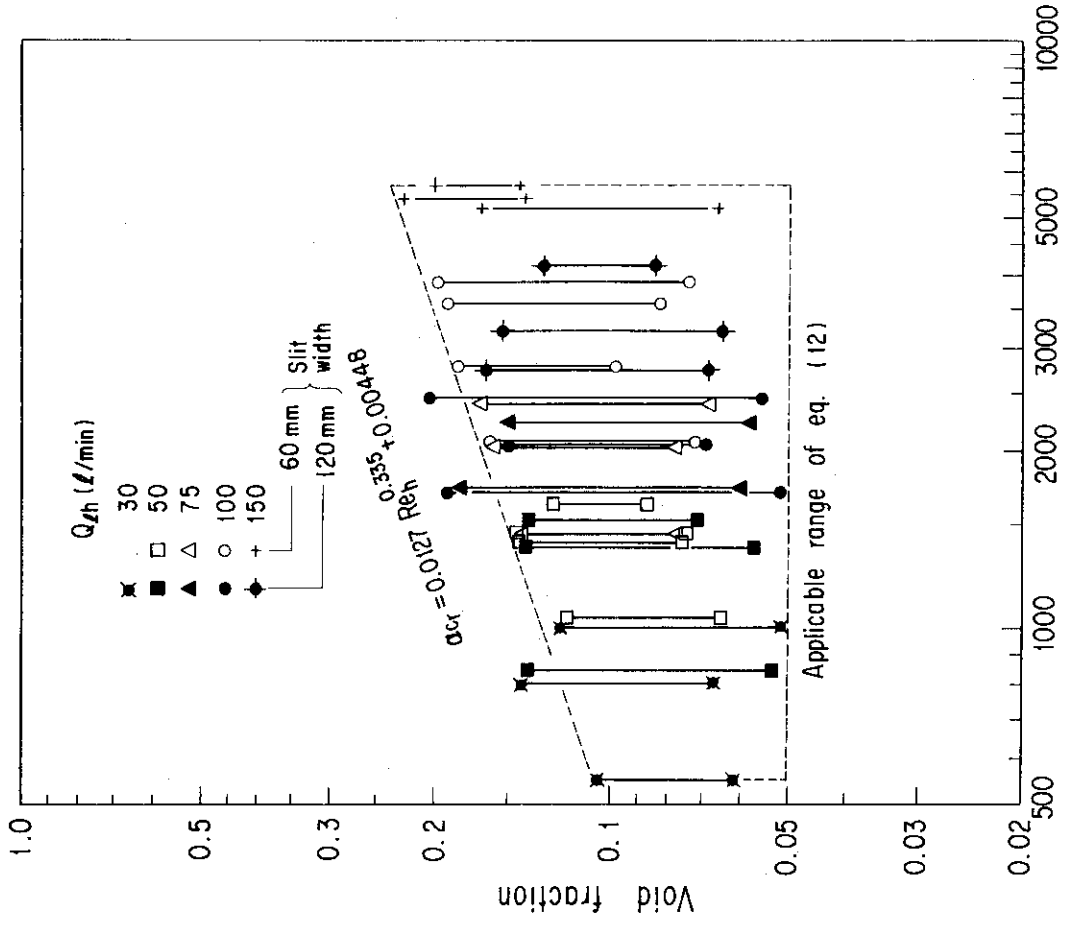

Fig. 3-21 Applicable ranges of void fraction and cross flow Reynolds number for cross flow resistance correlation

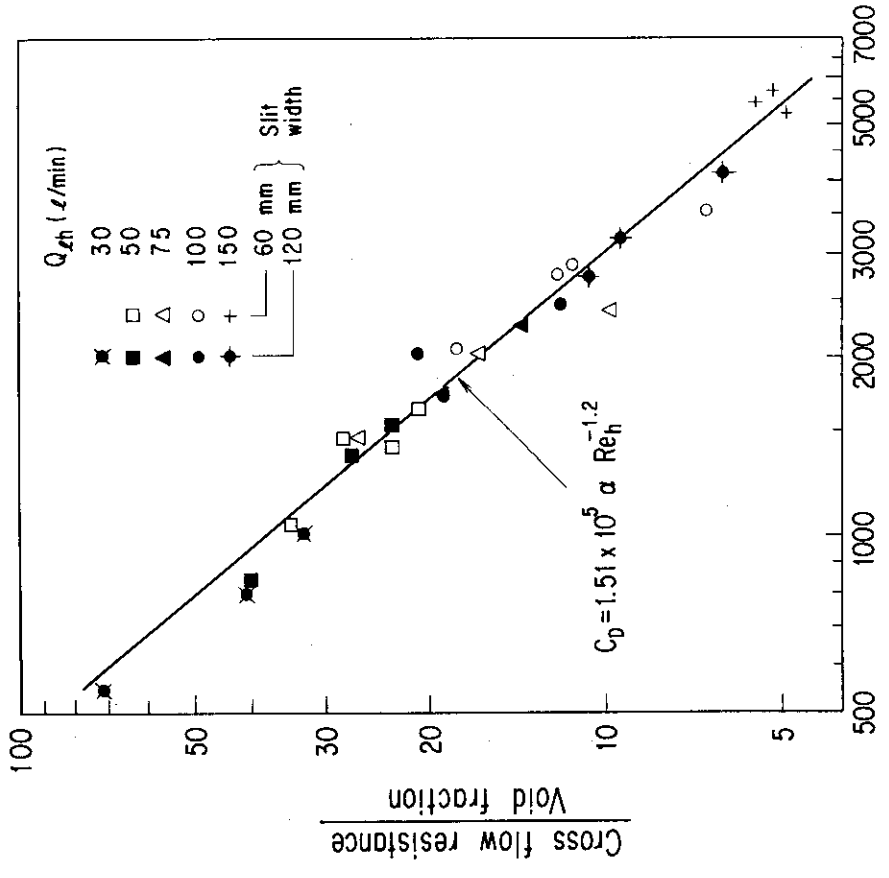

Fig. 3-20 Relation between cross flow resistance devided by void fraction and cross flow Reynolds number

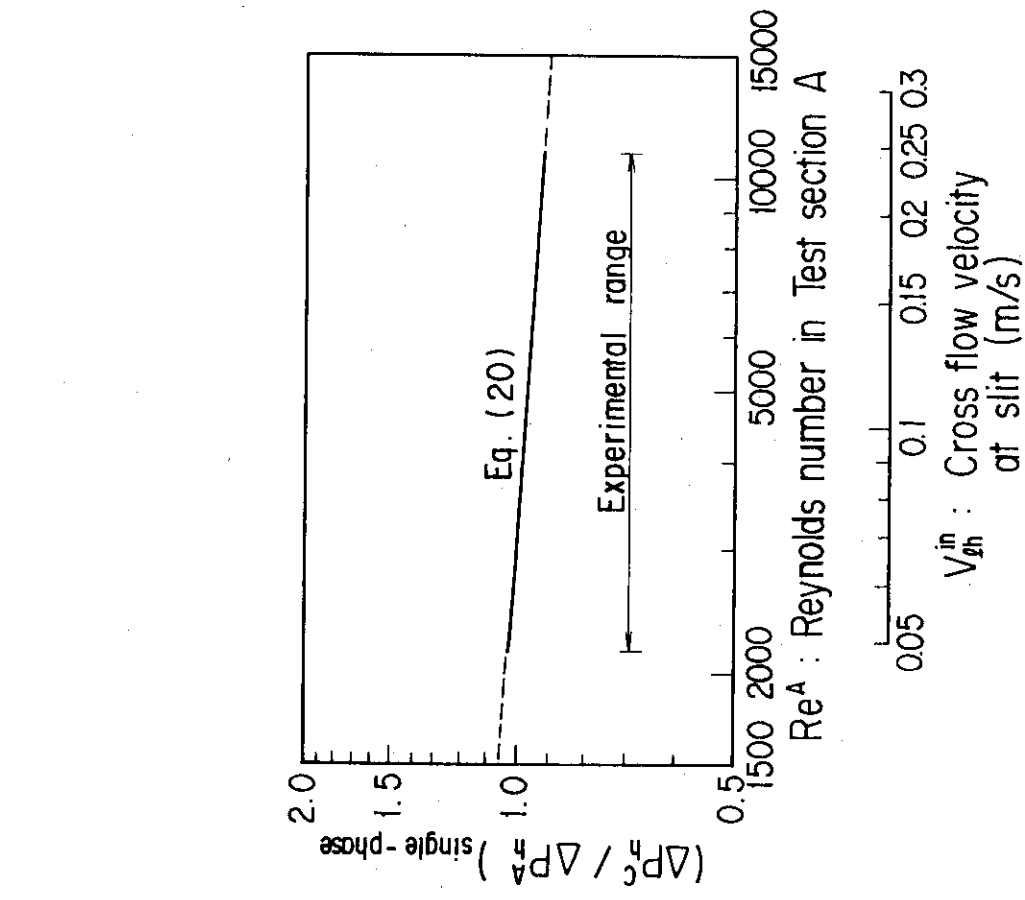

Fig. 3-23 Ratio of calculated horizontal differential pressure in single-phase cross flow between Test Sections C and A (attack angles: 45° and 90°) vs. cross flow Reynolds number

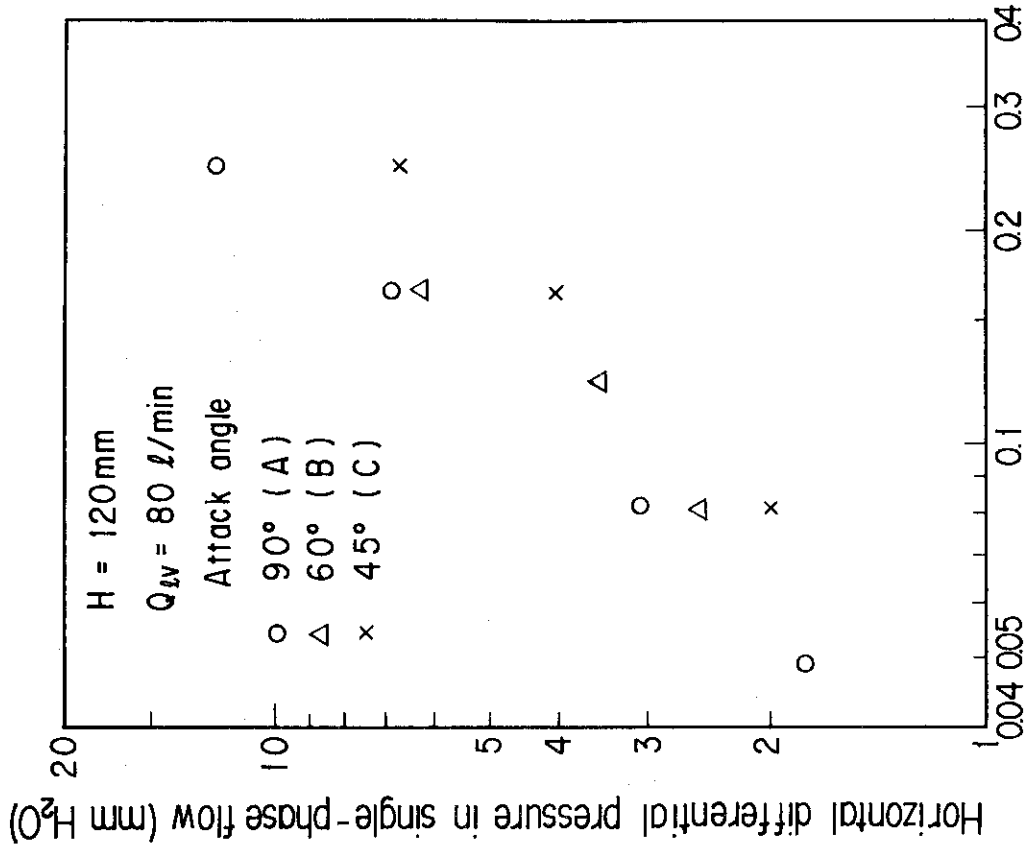

Fig. 3-22 Horizontal differential pressure in single-phase flow vs. cross flow velocity at slit in Test Sections A, B and C (attack angles: 90°, 60° and 45°)

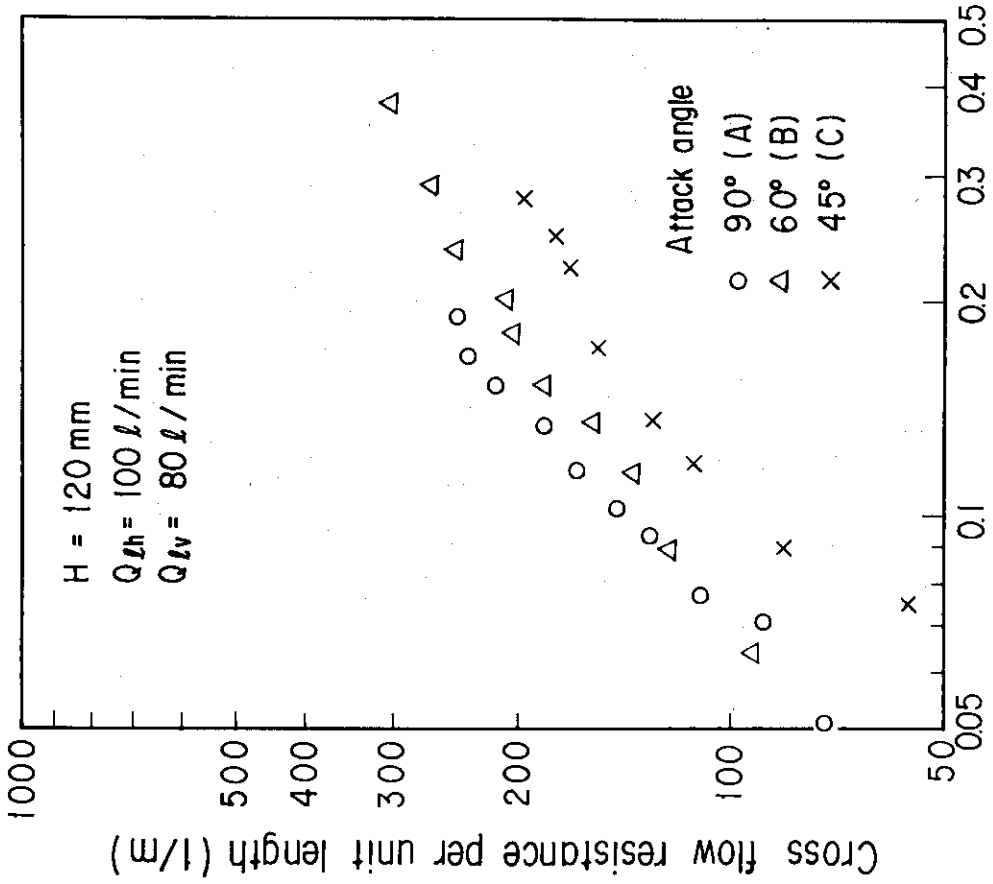

Fig. 3-25 Cross flow resistanve per unit length in Test Sections A, B and C vs. void fraction ($Q_{\ell h}$ = 100 ℓ/min)

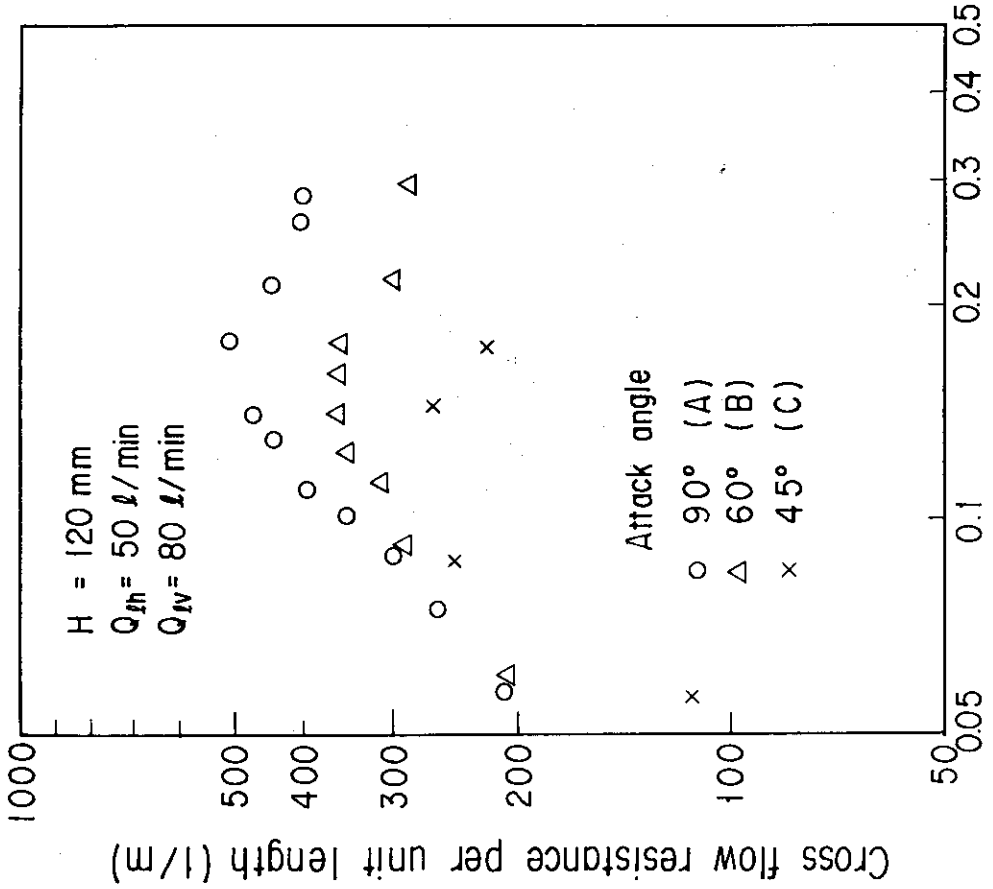

Fig. 3-24 Cross flow resistance per unit length in Test Sections A, B and C vs. void fraction ($Q_{\ell h}$ = 50 ℓ/min)

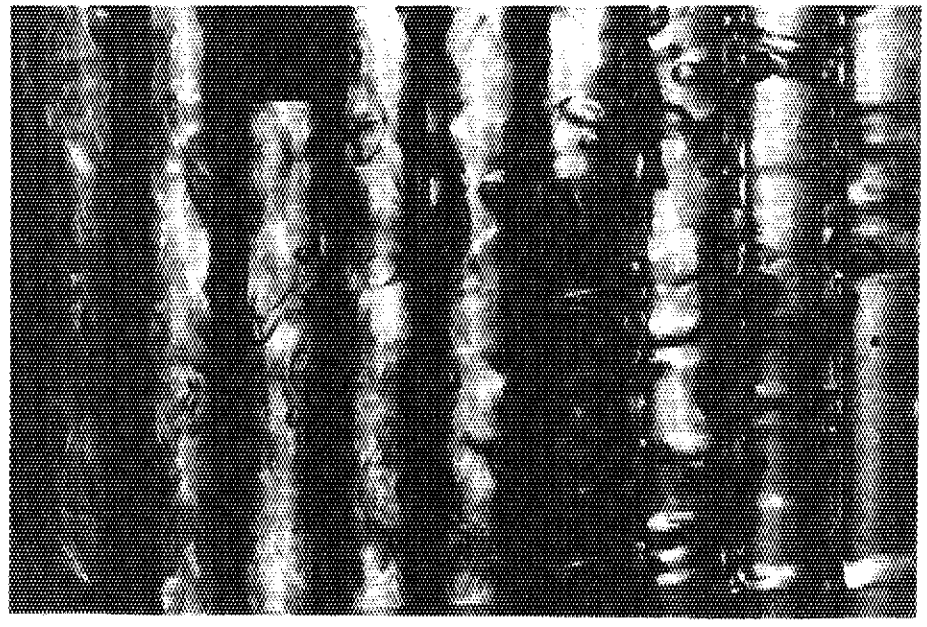

(a) Vgv = 0.0498 m/s

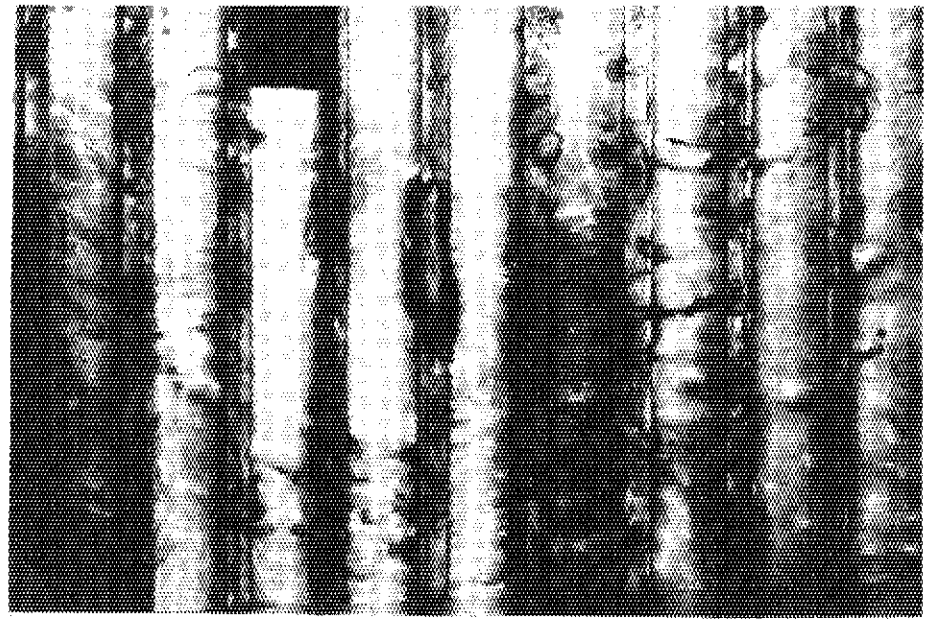

(b) Vgv = 0.398 m/s

Photo. 3-1 Two-phase flow pattern in rod bundle
(V_{lh0} = 0.373 m/s, V_{lv} = 0.0248 m/s)

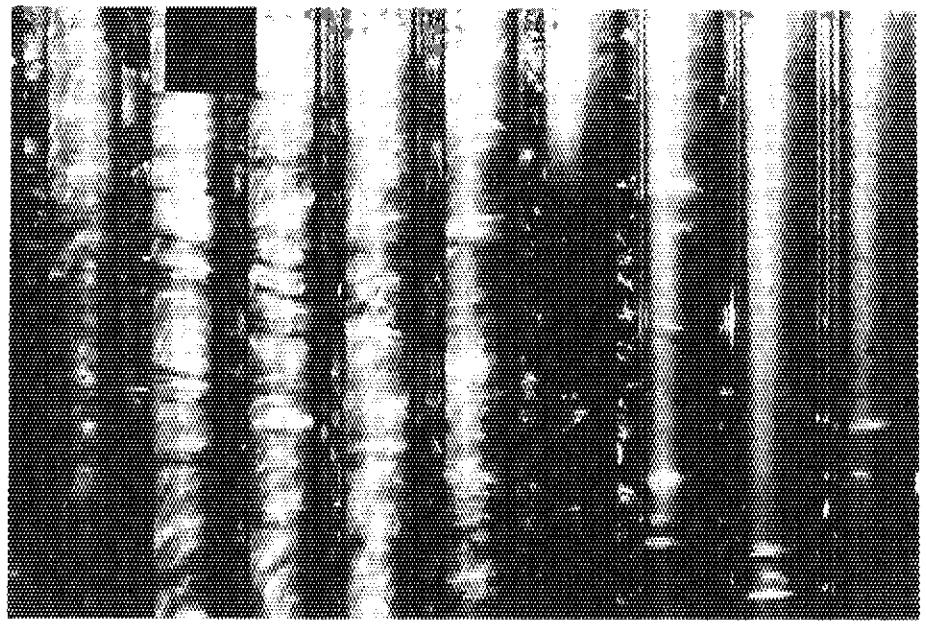

(a) Vgv = 0.0498 m/s

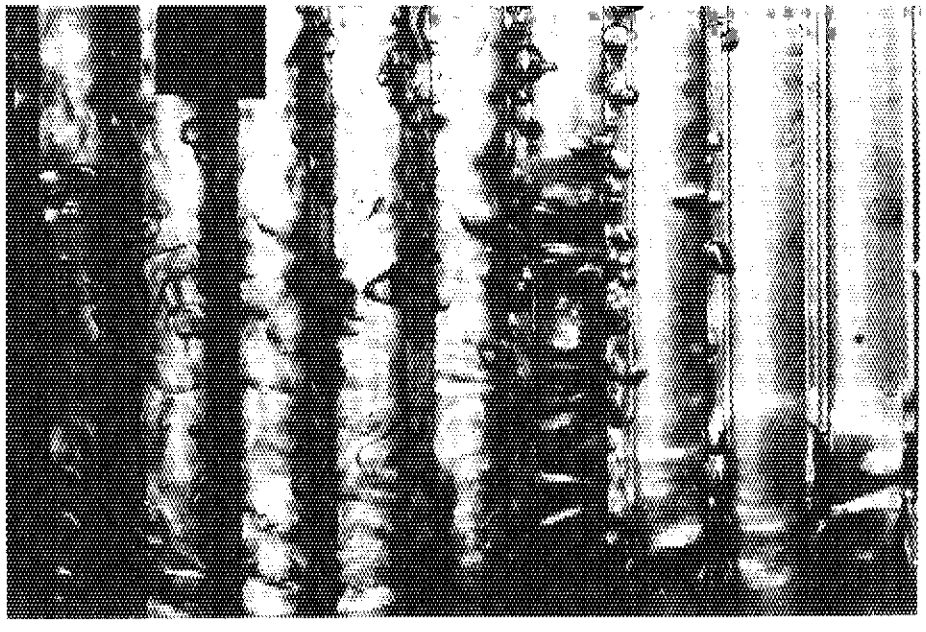

(b) Vgv = 0.398 m/s

Photo. 3-2 Two-phase flow pattern in rod bundle
(V_{lh0} = 0.747 m/s, V_{lv} = 0.0248 m/s)

4. CONCLUSIONS

A cross flow in a rod bundle in the presence of an air-water two-phase up-flow was experimentally studied to evaluate cross flow resistance during the reflood phase of a PWR-LOCA. The major results are as follows:

(1) The air cross flow rate was observed to be small in comparison to the air up-flow rate even under the condition of higher water cross flow rate than expected in the reflood phase.

(2) The estimated cross flow resistance increased in proportion to the void fraction up to a certain value (critical void fraction) and above that void fraction the cross flow resistance decreased with the void fraction. The occurrence of peak cross flow resistance at the critical void fraction is considered to be caused by the flow pattern transition from a bubbly flow to a slug flow. The critical void fraction increased with the cross flow velocity and the vertical superficial velocity. The critical void fraction was approximately expressed with the following correlation.

$$\alpha_{cr} = 0.0127\ Re_h^{0.335} + 0.0048$$

where $Re_h = \dfrac{\rho_\ell\ V_{\ell h}\ D_{rod}}{\mu_\ell}$

(3) Below the critical void fraction, cross flow resistance significantly decreased with the cross flow velocity. The effect of the cross flow velocity on the cross flow resistance was much larger in the two-phase flow than in the single-phase flow. A correlation of cross flow resistance was proposed as a function of the void fraction and the cross flow Reynolds number. The correlation is

$$C_D = 1.51 \times 10^5\ \alpha\ Re_h^{-1.2}$$

The applicable ranges of this correlation are

$$0.05 \leq \alpha \leq \alpha_{cr}, \text{ and } 550 \leq Re_h \leq 5640.$$

(4) The estimated cross flow resistance in a two-phase flow was much higher than the single-phase cross flow resistance which has been

used in two-dimensional safety analysis codes.

It should be noted here that the presented correlations of the critical void fraction and the cross flow resistance are applicable only for the square array of 10.7 mm rods with the pitch of 14.3 mm.

(5) The cross flow attack angle against the bundle lattice had little effect on the two-phase cross flow resistance.

ACKNOWLEDGMENT

The authors would like to express their gratitude to Dr. Y. Murao and Messrs. T. Okubo, A. Ohnuki and Y. Abe for discussions and suggestions.

used in two-dimensional safety analysis codes.

It should be noted here that the presented correlations of the critical void fraction and the cross flow resistance are applicable only for the square array of 10.7 mm rods with the pitch of 14.3 mm.

(5) The cross flow attack angle against the bundle lattice had little effect on the two-phase cross flow resistance.

ACKNOWLEDGMENT

The authors would like to express their gratitude to Dr. Y. Murao and Messrs. T. Okubo, A. Ohnuki and Y. Abe for discussions and suggestions.

NOMENCLATURE

C_D = cross flow resistance in two-phase flow
c_D^m = cross flow resistance in homogeneous model
C_D^s = cross flow resistance in single-phase flow
C_D^o = cross flow resistance per unit flow-directional length
D_{rod} = rod outer diameter
f = cross flow expansion factor
H = slit width
L_h = measurement span of horizontal differential pressure
N_T = number of rod
N_A = number of rods in L_h for Test Section A
N_c = number of rods in L_h for Test Section C
ΔP_h = horizontal differential pressure
ΔP_{ho} = horizontal differential pressure without flow expansion
ΔP_h^A = horizontal differential pressure in Test Section A
ΔP_h^B = horizontal differential pressure in Test Section B
ΔP_v = vertical differential pressure
$Q_{\ell h}$ = water cross flow rate
$Q_{\ell v}$ = vertical water flow rate
Q_{gv} = vertical air flow rate
Re_h = horizontal water Reynolds number given by eq. (5)
Re_h^A = cross flow Reynolds number in Test Section A
Re_h^B = cross flow Reynolds number in Test Section B
S = square pitch of rod bundle
T_ℓ = water temperature
V_{mh} = homogeneous cross flow velocity
$V_{\ell h}$ = water cross flow velocity
$V_{\ell ho}$ = water cross flow velocity without flow expansion
$V_{\ell h}^{in}$ = water cross flow velocity at slit
$V_{\ell h}^A$ = water cross flow velocity at gap between rods in Test Section A
$V_{\ell h}^C$ = water cross flow velocity at gap between rods in Test Section C
V_{gh} = air cross flow velocity
$V_{\ell v}$ = vertical superficial water velocity
V_{gv} = vertical superficial air velocity
α = void fraction
α_{cr} = critical void fraction

ρ_m = two-phase mixture density
ρ_ℓ = water density
ρ_g = air density
μ_ℓ = dynamic viscosity
ψ = cross flow attack angle

References

(1) H. Adachi et al., Design of Slab Core Test Facility (SCTF) in Large Scale Reflood Test Program, Part I: Core-I, JAERI-M 83-080, 1983.

(2) M. Sobajima et al., Design of Slab Core Test Facility (SCTF) in Large Scale Reflood Test Program, Part II: Core-II, JAERI-M to be published.

(3) T. Iwamura et al., Effects of Radial Core Power Profile on Core Thermo-Hydraulic Behavior during Reflood Phase in PWR-LOCA, J. Nucl. Sci. Tech., vol. 20, No. 9 pp. 743-751, 1983.

(4) T. Iwamura et al., Two-Dimensional Thermal-Hydraulic Behavior in Core in SCTF Core-II Cold Leg Injection Tests (Radial Power Profile Test Results), JAERI-M 85-106, 1985.

(5) M. Osakabe and H. Adachi, The Characteristics of Cross Flow in a Rod Bundle, JAERI-M 82-003, 1982.

(6) T. Iwamura and H. Adachi, Evaluation of Cross Flow Velocity across Rod Bundles during Reflood Phase in SCTF Core-I Forced-Feed Flooding Tests, Private Communication.

(7) C. W. Stewart, et al., COBRA-IV, The Model and the Method, BNWL-2214, 1977.

(8) J. Weisman, Cross Flow Resistance in Rod Bundle Cores, Nucl. Tech., vol. 15, pp. 465-469, 1972.

(9) M. Osakabe and H. Adachi, Characteristic of Two-Phase Slanting Flow in Rod Bundle, J. Nucl. Sci. Tech. vol. 19, No. 6, pp. 504-506, 1982.

(10) Idel'chik, Handbook of Hydraulic Resistance, AEC-tr-6630 (translated from Russian), 1966

APPENDIX TEST RESULTS

Table A-1 Single-phase cross flow test results

(a) Slit width = 30 mm

$Q_{\ell h}$ (ℓ/min)	$V_{\ell ho}$ (m/s)	ΔP_{ho} (mmH_2O)	$Q_{\ell v}$ (ℓ/min)	$V_{\ell v}$ (m/s)	ΔP_h (mmH_2O)	f	$V_{\ell h}$ (m/s)
50	1.49	568	15	0.0248	2.6	14.8	0.101
			35	0.0580	3.8	12.2	0.122
			80	0.132	3.5	12.7	0.117
100	2.99	2270	15	0.0248	6.0	19.5	0.153
			35	0.0580	4.2	23.2	0.129

(b) Slit width = 60 mm

$Q_{\ell h}$ (ℓ/min)	$V_{\ell ho}$ (m/s)	ΔP_{ho} (mmH_2O)	$Q_{\ell v}$ (ℓ/min)	$V_{\ell v}$ (m/s)	ΔP_h (mmH_2O)	f	$V_{\ell h}$ (m/s)
30	0.448	51	15	0.0248	1.4	6.04	0.074
			35	0.0580	1.4	6.04	0.074
			80	0.132	1.6	5.65	0.079
			150	0.248	2.0	5.05	0.089
40	0.597	91	15	0.0248	1.6	7.54	0.079
			35	0.0580	1.6	7.54	0.079
			80	0.132	1.8	7.11	0.084
			150	0.248	2.1	6.58	0.091
50	0.747	142	15	0.0248	2.3	7.86	0.095
			35	0.0580	3.0	6.88	0.109
			80	0.132	2.3	7.86	0.095
			150	0.248	3.0	6.88	0.109
60	0.896	205	15	0.0248	2.5	9.05	0.099
			35	0.0580	2.3	9.44	0.095
			80	0.132	3.2	8.00	0.112
			150	0.248	3.2	8.00	0.112

$Q_{\ell h}$ (ℓ/min)	$V_{\ell ho}$ (m/s)	ΔP_{ho} (mmH_2O)	$Q_{\ell v}$ (ℓ/min)	$Q_{\ell v}$ (ℓ/min)	ΔP_h (mmH_2O)	f	$V_{\ell h}$ (m/s)
75	1.120	320	15	0.0248	3.0	10.3	0.109
			35	0.0580	3.9	9.06	0.124
			80	0.132	7.4	6.58	0.170
			150	0.248	4.7	8.25	0.136
80	1.19	364	15	0.0248	3.8	9.79	0.122
			35	0.0580	4.1	9.42	0.126
			80	0.132	8.4	6.58	0.181
			150	0.248	5.3	8.29	0.144
100	1.49	568	15	0.0248	7.3	8.82	0.169
			35	0.0580	7.5	8.70	0.171
			80	0.132	13.1	6.59	0.226
			150	0.248	11.9	6.91	0.216
120	1.79	819	15	0.0248	17.2	6.90	0.259
			35	0.0580	17.1	6.92	0.259
			80	0.132	17.9	6.84	0.262
			150	0.248	17.5	6.76	0.265
140	2.09	1115	15	0.0248	22.8	6.99	0.299
			35	0.0580	22.8	6.99	0.299
			80	0.132	23.4	6.90	0.303
			150	0.248	24.3	6.77	0.309
150	2.24	1280	15	0.0248	27.1	6.87	0.326
			35	0.0580	26.4	6.96	0.322
			80	0.132	26.2	6.99	0.320
			150	0.248	27.3	6.85	0.327
160	2.39	1455	15	0.0248	28.6	7.13	0.335
			35	0.0580	28.4	7.16	0.334
			80	0.132	28.9	7.10	0.337
			150	0.248	31.2	6.83	0.350

(c) Slit width = 120 mm

$Q_{\ell h}$ (ℓ/min)	$V_{\ell ho}$ (m/s)	ΔP_{ho} (mmH_2O)	$Q_{\ell v}$ (ℓ/min)	$V_{\ell v}$ (m/s)	ΔP_h (mmH_2O)	f	$V_{\ell h}$ (m/s)
30	0.224	17.8	15	0.0248	1.1	4.02	0.056
			35	0.0580	1.2	3.85	0.058
			80	0.132	1.8	3.14	0.071
			150	0.248	2.3	2.78	0.081
50	0.373	35.6	15	0.0248	2.2	4.02	0.093
			35	0.0580	2.6	3.70	0.101
			80	0.132	3.1	3.39	0.110
			150	0.248	3.7	3.10	0.120
75	0.560	80.0	15	0.0248	3.9	4.53	0.124
			35	0.0580	4.2	4.36	0.128
			80	0.132	5.4	3.85	0.145
			150	0.248	7.2	3.33	0.168
100	0.747	142.2	15	0.0248	6.4	4.71	0.158
			35	0.0580	7.0	4.50	0.166
			80	0.132	7.0	4.50	0.166
			150	0.248	10.9	3.61	0.207
150	1.12	319.9	15	0.0248	11.0	5.39	0.208
			35	0.0580	10.2	5.60	0.200
			80	0.132	12.5	5.06	0.221
			150	0.248	18.5	4.16	0.269

Table A-2 Two-phase cross flow test results
(Slit width = 30 mm)

(1) $Q_{\ell h}$ = 50 ℓ/min, $V_{\ell ho}$ = 1.49 m/s

$Q_{\ell v}$ (ℓ/min)	$V_{\ell v}$ (m/s)	f	$V_{\ell h}$ (m/s)	Q_{gv} (ℓ/min)	V_{gv} (m/s)	ΔP_h (mmH_2O)	α	C_D
15	0.0248	14.8	0.107	21.6	0.0356	12.0	0.056	2.33
				43.2	0.0712	14.1	0.092	2.73
				86.3	0.142	16.5	0.111	3.19
				129	0.214	16.8	0.133	3.24
				173	0.285	15.2	0.163	2.94
				259	0.427	15.0	0.202	2.90
				345	0.570	7.8	0.233	1.51
				432	0.712	12.3	0.256	2.38
				518	0.854	9.0	0.265	1.73
				690	1.14	7.2	0.320	1.40
35	0.0580	12.2	0.122	21.6	0.0356	12.0	0.058	1.58
				34.5	0.0570	12.6	0.083	1.65
				43.2	0.0712	15.6	0.086	2.05
				51.8	0.0854	16.2	0.111	2.13
				86.3	0.142	17.1	0.117	2.25
				173	0.285	19.2	0.156	2.52
				259	0.427	16.8	0.189	2.21
				432	0.712	16.8	0.222	2.20
				518	0.854	12.0	0.256	1.58
				690	1.14	10.8	0.289	1.42
80	0.132	12.7	0.117	21.6	0.0356	11.4	0.039	1.63
				34.5	0.0570	12.3	0.081	1.75
				43.2	0.0712	14.4	0.083	2.06
				78.5	0.129	15.9	0.109	2.27
				86.3	0.142	16.8	0.100	2.39
				129	0.214	17.4	0.127	2.48
				173	0.285	19.2	0.133	2.74
				259	0.427	19.8	0.147	2.82
				432	0.712	19.2	0.169	2.74
				518	0.854	18.6	0.200	2.65

(2) $Q_{\ell h}$ = 100 ℓ/min, $V_{\ell ho}$ = 2.99 m/s

$Q_{\ell v}$ (ℓ/min)	$V_{\ell v}$ (m/s)	f	$V_{\ell h}$ (m/s)	Q_{gv} (ℓ/min)	V_{gv} (m/s)	ΔP_h (mmH_2O)	α	C_D
15	0.0248	19.5	0.153	21.6	0.0356	12.6	0.040	1.05
				43.2	0.0712	19.2	0.069	1.60
				86.3	0.142	24.9	0.103	2.08
				129	0.214	29.4	0.120	2.46
				173	0.285	32.7	0.129	3.28
				302	0.499	36.0	0.144	3.00
				432	0.712	33.9	0.160	2.82
35	0.0580	23.2	0.129	21.6	0.0356	12.0	0.080	1.42
				43.2	0.0712	16.8	0.111	1.97
				86.3	0.142	25.2	0.128	2.97
				129	0.214	28.8	0.139	3.40
				173	0.285	31.2	0.134	3.68
				259	0.427	34.2	0.164	4.04
				345	0.570	36.0	0.180	4.25
				432	0.712	35.7	0.201	4.21

Table A-3 Two-phase cross flow test results
(Slit width = 60 mm)

* = data points used for developing a cross flow resistance correlation

(1) $Q_{\ell h}$ = 30 ℓ/min, $V_{\ell ho}$ = 0.448 m/s

$Q_{\ell v}$ (ℓ/min)	$V_{\ell v}$ (m/s)	f	$V_{\ell h}$ (m/s)	Q_{gv} (ℓ/min)	V_{gv} (m/s)	ΔP_h (mmH_2O)	α	C_D
15	0.0248	6.04	0.074	17.3	0.0285	9.0	0.066	3.21
T_ℓ = 13 °C				43.2	0.0712	9.5	0.110	3.39
$\mu_\ell = 1.22\times10^{-3}$ Pa·s				86.3	0.142	6.3	0.132	2.25
Re_h = 650				173	0.285	6.3	0.200	2.25
80	0.132	5.65	0.079	17.3	0.0285	6.4	0.046	2.00
T_ℓ = 15 °C				43.2	0.0712	8.8	0.087	2.74
$\mu_\ell = 1.16\times10^{-3}$ Pa·s				86.3	0.142	9.3	0.121	2.91
Re_h = 730				173	0.285	8.6	0.154	2.69
				345	0.570	4.0	0.209	1.25
150	0.248	5.05	0.089	17.3	0.0285	6.5	0.036	1.62
T_ℓ = 17 °C				43.2	0.0712	8.0	0.083	1.99
$\mu_\ell = 1.10\times10^{-3}$ Pa·s				86.3	0.142	10.3	0.114	2.56
Re_h = 860				173	0.285	9.4	0.132	2.34
				345	0.570	8.7	0.165	2.16
				518	0.854	6.3	0.215	1.57

(2) $Q_{\ell h}$ = 50 ℓ/min, $V_{\ell ho}$ = 0.747 m/s

$Q_{\ell v}$ (ℓ/min)	$V_{\ell v}$ (m/s)	f	$V_{\ell h}$ (m/s)	Q_{gv} (ℓ/min)	V_{gv} (m/s)	ΔP_h (mmH_2O)	α	C_D	
15	0.0248	7.86	0.095	17.3	0.0285	11.5	0.065	2.50	*
T_ℓ = 21 °C				34.3	0.0570	15.0	0.086	3.25	*
$\mu_\ell = 0.98\times10^{-3}$ Pa·s				43.2	0.0715	16.8	0.101	3.65	*
Re_h = 1040				69.0	0.114	15.6	0.105	3.18	*
				86.3	0.142	16.5	0.115	3.58	*

$Q_{\ell v}$ (ℓ/min)	$V_{\ell v}$ (m/s)	f	$V_{\ell h}$ (m/s)	Q_{gv} (ℓ/min)	V_{gv} (m/s)	ΔP_h (mmH_2O)	α	C_D	
				129	0.214	19.0	0.119	4.13	*
				173	0.285	13.9	0.151	3.02	
				345	0.570	11.0	0.206	2.39	
35	0.0580	6.88	0.109	17.3	0.0285	8.8	0.063	0.87	
				34.5	0.0570	11.8	0.087	1.97	*
T_ℓ = 35 °C				69.0	0.114	12.8	0.109	2.13	*
$\mu_\ell = 0.72\times10^{-3}$ Pa·s				129	0.214	14.5	0.120	2.42	*
Re_h = 1620				173	0.285	15.2	0.125	2.53	*
				345	0.570	10.2	0.196	1.70	
				690	1.14	8.0	0.272	1.33	
80	0.132	7.86	0.095	17.3	0.0285	9.3	0.061	2.02	
				34.5	0.0570	10.4	0.076	2.26	*
T_ℓ = 37 °C				43.2	0.0712	11.8	0.089	2.56	*
$\mu_\ell = 0.70\times10^{-3}$ Pa·s				69.0	0.114	12.8	0.098	2.78	*
Re_h = 1450				129	0.214	16.0	0.125	3.47	*
				173	0.285	15.9	0.144	3.46	*
				259	0.427	14.4	0.154	3.13	
				432	0.712	13.8	0.175	2.99	
				518	0.854	9.6	0.228	2.09	
				690	1.14	6.7	0.263	1.46	
150	0.248	6.88	0.109	17.3	0.0285	9.0	0.037	1.50	
				34.5	0.0570	10.0	0.075	1.66	*
T_ℓ = 28 °C				43.2	0.0712	12.0	0.082	2.00	*
$\mu_\ell = 0.83\times10^{-3}$ Pa·s				69.0	0.114	14.2	0.097	2.36	*
Re_h = 1400				86.3	0.142	15.2	0.108	2.53	*
				129	0.214	16.0	0.117	2.66	*
				173	0.285	17.2	0.118	2.86	*
				345	0.570	18.3	0.146	3.04	*
				432	0.712	17.6	0.161	2.93	
				518	0.854	19.7	0.171	3.28	
				690	1.14	19.0	0.187	3.16	

(3) $Q_{\ell h}$ = 75 ℓ/min, $V_{\ell ho}$ = 1.12 m/s

$Q_{\ell v}$ (ℓ/min)	$V_{\ell v}$ (m/s)	f	$V_{\ell h}$ (m/s)	Q_{gv} (ℓ/min)	V_{gv} (m/s)	ΔP_h (mmH_2O)	α	C_D	
15	0.0248	10.3	0.109	17.3	0.0285	13.4	0.078	2.21	*
				43.2	0.0712	15.2	0.111	2.53	*
T_ℓ = 30 °C				86.3	0.142	20.2	0.123	3.35	*
$\mu_\ell = 0.80\times10^{-3}$ Pa·s				173	0.285	23.4	0.127	3.88	*
Re_h = 1450				345	0.570	19.8	0.143	3.28	*
				518	0.854	19.6	0.200	3.25	
80	0.132	6.58	0.170	17.3	0.0285	10.7	0.047	0.72	
				30.2	0.0498	13.4	0.068	0.69	*
T_ℓ = 32 °C				43.2	0.0712	15.8	0.102	1.07	*
$\mu_\ell = 0.76\times10^{-3}$ Pa·s				86.3	0.142	18.1	0.124	1.22	*
Re_h = 2400				173	0.285	22.9	0.155	1.55	*
				345	0.570	23.7	0.167	1.60	*
				518	0.854	23.0	0.167	1.56	*
150	0.248	8.25	0.136	17.3	0.0285	8.0	0.039	0.79	
				43.2	0.0712	13.7	0.078	1.36	*
T_ℓ = 35 °C				86.3	0.142	17.0	0.103	1.67	*
$\mu_\ell = 0.72\times10^{-3}$ Pa·s				173	0.285	20.9	0.123	2.05	*
Re_h = 2020				345	0.570	23.6	0.146	2.32	*
				518	0.854	25.6	0.159	2.51	*

(4) $Q_{\ell h}$ = 100 ℓ/min, $V_{\ell ho}$ = 1.49 m/s

$Q_{\ell v}$ (ℓ/min)	$V_{\ell v}$ (m/s)	f	$V_{\ell h}$ (m/s)	Q_{gv} (ℓ/min)	V_{gv} (m/s)	ΔP_h (mmH_2O)	α	C_D	
15	0.0248	8.82	0.169	17.3	0.0285	15.4	0.098	1.05	*
				34.5	0.0570	18.9	0.096	1.30	*
T_ℓ = 41 °C				86.3	0.142	22.8	0.128	1.57	*
$\mu_\ell = 0.65\times10^{-3}$ Pa·s				173	0.285	26.0	0.133	1.79	*
Re_h = 2780				518	0.854	31.5	0.181	2.17	*

$Q_{\ell v}$ (ℓ/min)	$V_{\ell v}$ (m/s)	f	$V_{\ell h}$ (m/s)	Q_{gv} (ℓ/min)	V_{gv} (m/s)	ΔP_h (mmH_2O)	α	C_D	
35	0.0580	8.70	0.179	17.3	0.0285	23.4	0.072	1.56	*
T_ℓ = 25 °C				43.2	0.0712	27.2	0.105	1.82	*
$\mu_\ell = 0.89\times10^{-3}$ Pa·s				86.3	0.142	31.9	0.117	2.13	*
Re_h = 2060				173	0.285	34.4	0.136	2.30	*
				345	0.570	37.6	0.140	2.52	*
				432	0.712	36.3	0.160	2.43	*
				690	1.14	32.0	0.179	2.14	
80	0.132	6.59	0.226	34.5	0.0570	14.0	0.083	0.54	*
T_ℓ = 37 °C				86.3	0.142	21.9	0.148	0.84	*
$\mu_\ell = 0.68\times10^{-3}$ Pa·s				173	0.285	31.5	0.160	1.21	*
Re_h = 3560				518	0.854	34.6	0.190	1.33	*
150	0.248	6.91	0.216	34.5	0.0570	19.8	0.054	0.83	
T_ℓ = 30 °C				43.2	0.0712	22.4	0.074	0.95	*
$\mu_\ell = 0.80\times10^{-3}$ Pa·s				51.8	0.0854	22.5	0.076	0.95	*
Re_h = 2890				69.0	0.114	25.6	0.085	1.08	*
				86.3	0.142	25.7	0.098	1.09	*
				129	0.214	28.0	0.108	1.18	*
				173	0.285	31.7	0.121	1.34	*
				345	0.570	36.6	0.143	1.54	*
				432	0.712	42.1	0.157	1.78	*
				518	0.854	43.2	0.169	1.83	*
				604	0.997	45.6	0.174	1.93	*
				690	1.14	45.4	0.198	1.91	*

(5) $Q_{\ell h}$ = 150 ℓ/min, $V_{\ell ho}$ = 2.24 m/s

$Q_{\ell v}$ (ℓ/min)	$V_{\ell v}$ (m/s)	f	$V_{\ell v}$ (m/s)	Q_{gv} (ℓ/min)	V_{gv} (m/s)	ΔP_h (mmH_2O)	α	C_D	
15	0.0248	6.87	0.326	17.3	0.0285	31.1	0.066	0.574	*
T_ℓ = 39 °C				43.2	0.0712	32.8	0.115	0.605	*
$\mu_\ell = 0.67\times10^{-3}$ Pa·s				86.3	0.142	35.6	0.134	0.656	*
Re_h = 5200				173	0.285	36.7	0.143	0.678	*

$Q_{\ell v}$ (ℓ/min)	$V_{\ell v}$ (m/s)	f	$V_{\ell h}$ (m/s)	Q_{gv} (ℓ/min)	V_{gv} (m/s)	ΔP_h (mmH_2O)	α	C_D	
				345	0.570	41.9	0.166	0.773	*
80	0.132	6.99	0.320	30.2	0.0498	32.0	0.065	0.611	
T_ℓ = 41 °C				43.2	0.0712	37.1	0.107	0.708	
$\mu_\ell = 0.64\times10^{-3}$ Pa·s				86.3	0.142	41.2	0.140	0.787	*
Re_h = 5350				173	0.285	46.0	0.153	0.864	*
				345	0.570	52.2	0.194	1.00	*
				518	0.854	53.8	0.224	1.02	*
150	0.248	6.85	0.327	43.2	0.0712	28.1	0.041	0.515	
T_ℓ = 43 °C				69.0	0.114	34.6	0.055	0.634	
$\mu_\ell = 0.62\times10^{-3}$ Pa·s				86.3	0.142	35.7	0.061	0.655	
Re_h = 5640				173	0.285	44.3	0.147	0.812	*
				345	0.570	52.0	0.191	0.951	*
				518	0.854	54.8	0.198	1.01	*

Table A-4 Two-phase cross flow test results
(Slit width = 120 mm)

* = data points used for developing a cross flow resistance correlation

(1) $Q_{\ell h}$ = 30 ℓ/min, $V_{\ell ho}$ = 0.224 m/s

$Q_{\ell v}$ (ℓ/min)	$V_{\ell v}$ (m/s)	f	$V_{\ell h}$ (m/s)	Q_{gv} (ℓ/min)	V_{gv} (m/s)	ΔP_h (mmH_2O)	α	C_D	
15	0.0248	4.02	0.056	17.3	0.0285	7.8	0.062	4.92	*
				30.2	0.0498	10.2	0.090	6.44	*
T_ℓ = 17 °C				43.2	0.0712	11.0	0.105	6.95	*
μ_ℓ = 1.09 × 10^{-3} Pa.s				86.3	0.142	10.8	0.129	6.82	
Re_h = 550				129	0.214	9.3	0.163	5.88	
				173	0.285	7.8	0.205	4.93	
				345	0.570	7.0	0.259	4.42	
80	0.132	3.14	0.071	17.3	0.0285	2.3	0.043	0.89	
				30.2	0.0498	7.0	0.067	2.70	*
				43.2	0.0712	9.8	0.086	3.77	*
T_ℓ = 22 °C				86.3	0.142	12.9	0.118	4.98	*
μ_ℓ = 0.96 × 10^{-3} Pa.s				129	0.214	14.0	0.141	5.39	*
Re_h = 800				173	0.285	12.6	0.168	4.86	
				345	0.570	11.5	0.223	4.43	
				518	0.854	8.2	0.272	3.16	
				690	1.14	6.6	0.314	2.55	
150	0.248	2.78	0.082	17.3	0.0285	5.6	0.051	1.70	*
				30.2	0.0498	7.2	0.063	2.17	*
				43.2	0.0712	8.6	0.084	2.59	*
T_ℓ = 27 °C				86.3	0.142	12.2	0.104	3.69	*
μ_ℓ = 0.85 × 10^{-3} Pa.s				129	0.214	12.6	0.128	3.81	*
Re_h = 1010				173	0.285	13.1	0.122	3.95	*
				345	0.570	13.3	0.182	4.02	
				518	0.854	12.4	0.206	3.75	
				690	1.14	10.3	0.248	3.11	
				863	1.42	8.7	0.272	3.62	

(2) $Q_{\ell h}$ = 50 ℓ/min, $V_{\ell ho}$ = 0.373 m/s

$Q_{\ell v}$ (ℓ/min)	$V_{\ell v}$ (m/s)	f	$V_{\ell h}$ (m/s)	Q_{gv} (ℓ/min)	V_{gv} (m/s)	ΔP_h (mmH_2O)	α	C_D	
15	0.0248	4.02	0.091	17.3	0.0285	9.8	0.053	2.23	*
				30.2	0.0498	14.3	0.074	3.25	*
T_ℓ = 14 °C				43.2	0.0712	16.4	0.084	3.73	*
μ_ℓ = 1.18×10^{-3} Pa·s				86.3	0.142	17.0	0.101	3.87	*
Re_h = 840				129	0.214	22.2	0.117	5.06	*
				173	0.285	20.1	0.138	4.58	*
				345	0.570	16.6	0.200	3.78	
				518	0.854	11.7	0.254	2.66	
80	0.132	3.39	0.110	17.3	0.0285	10.1	0.057	1.63	*
				30.2	0.0498	12.6	0.075	2.04	*
				43.2	0.0712	14.7	0.088	2.38	*
				69.0	0.114	17.0	0.102	2.75	*
T_ℓ = 26 °C				86.3	0.142	19.2	0.110	3.11	*
μ_ℓ = 0.86×10^{-3} Pa·s				129	0.214	21.3	0.130	3.45	*
Re_h = 1370				173	0.285	22.7	0.139	3.67	*
				345	0.570	24.3	0.182	3.93	
				518	0.854	21.2	0.215	3.43	
				690	1.14	19.6	0.268	3.17	
				863	1.42	19.6	0.288	3.17	
150	0.248	3.10	0.120	17.3	0.0285	9.3	0.032	1.26	
				43.2	0.0712	12.4	0.072	1.68	*
				69.0	0.114	16.0	0.084	2.17	*
T_ℓ = 27 °C				86.3	0.142	17.1	0.092	2.32	*
μ_ℓ = 0.85×10^{-3} Pa·s				129	0.214	19.3	0.117	2.61	*
Re_h = 1510				173	0.285	20.7	0.118	2.80	*
				345	0.570	22.0	0.138	2.98	*
				518	0.854	23.5	0.170	3.19	
				690	1.14	24.9	0.190	3.37	
				863	1.42	27.2	0.222	3.69	

(3) $Q_{\ell h}$ = 75 ℓ/min, $V_{\ell ho}$ = 0.560 m/s

$Q_{\ell v}$ (ℓ/min)	$V_{\ell v}$ (m/s)	f	$V_{\ell h}$ (m/s)	Q_{gv} (ℓ/min)	V_{gv} (m/s)	ΔP_h (mmH_2O)	α	C_D	
15	0.0248	4.53	0.124	30.2	0.0498	19.3	0.012	2.48	
				43.2	0.0712	20.4	0.033	2.62	
				69.0	0.114	22.9	0.066	2.94	
T_ℓ = 19 °C				86.3	0.142	23.6	0.069	3.03	
μ_ℓ = 1.03×10^{-3} Pa·s				129	0.214	26.4	0.101	3.39	
Re_h = 1290				173	0.285	29.2	0.148	3.75	
				345	0.570	32.0	0.212	4.11	
				518	0.854	31.4	0.278	4.03	
				690	1.14	31.2	0.340	4.00	
80	0.132	3.85	0.145	30.2	0.0498	14.8	0.061	1.37	*
				43.2	0.0712	18.2	0.084	1.69	*
				69.0	0.114	21.8	0.110	2.02	*
T_ℓ = 25 °C				86.3	0.142	23.0	0.110	2.13	*
μ_ℓ = 0.89×10^{-3} Pa·s				129	0.214	26.2	0.131	2.43	*
Re_h = 1740				173	0.285	28.7	0.180	2.66	*
				345	0.570	33.1	0.238	3.07	
				518	0.854	35.1	0.275	3.25	
				690	1.14	35.5	0.302	3.29	
150	0.248	3.33	0.168	17.3	0.0285	10.8	0.024	0.75	
				30.2	0.0498	14.0	0.058	0.97	*
				43.2	0.0712	16.4	0.068	1.14	*
				69.0	0.114	18.1	0.089	1.26	*
T_ℓ = 30 °C				86.3	0.142	20.2	0.102	1.40	*
μ_ℓ = 0.8×10^{-3} Pa·s				129	0.214	24.2	0.116	1.68	*
Re_h = 2250				173	0.285	25.9	0.134	1.80	*
				345	0.570	28.6	0.149	1.98	*
				518	0.854	33.6	0.199	2.33	
				690	1.14	37.1	0.215	2.57	
				863	1.42	38.2	0.220	2.65	

(4) $Q_{\ell h}$ = 100 ℓ/min, $V_{\ell ho}$ = 0.747 m/s

$Q_{\ell v}$ (ℓ/min)	$V_{\ell v}$ (m/s)	f	$V_{\ell h}$ (m/s)	Q_{gv} (ℓ/min)	V_{gv} (m/s)	ΔP_h (mmH_2O)	α	C_D	
15	0.0248	4.71	0.158	17.3	0.0285	18.8	0.069	1.47	*
				30.2	0.0498	21.3	0.075	1.66	*
				43.2	0.0712	24.4	0.088	1.91	*
T_ℓ = 29 °C				86.3	0.142	28.3	0.104	2.21	*
μ_ℓ = 0.82×10^{-3} Pa·s				173	0.285	32.4	0.128	2.53	*
Re_h = 2060				345	0.570	37.4	0.147	2.92	*
				518	0.854	39.5	0.167	3.08	
				690	1.14	42.2	0.191	3.30	
80	0.132	4.50	0.166	17.3	0.0285	14.0	0.051	1.00	*
				30.2	0.0498	17.1	0.072	1.22	*
				43.2	0.0712	21.1	0.078	1.51	*
				69.0	0.114	25.1	0.095	1.79	*
T_ℓ = 19 °C				86.3	0.142	27.7	0.103	1.98	*
μ_ℓ = 1.03×10^{-3} Pa·s				129	0.214	31.1	0.117	2.22	*
Re_h = 1720				173	0.285	35.0	0.135	2.49	*
				345	0.570	40.6	0.155	2.90	*
				518	0.854	44.5	0.171	3.18	*
				690	1.14	45.8	0.192	3.27	*
150	0.248	3.61	0.207	30.2	0.0498	16.4	0.045	0.75	
				43.2	0.0712	18.6	0.056	0.85	*
				69.0	0.114	21.2	0.076	0.97	*
				86.3	0.142	23.8	0.088	1.09	*
T_ℓ = 24 °C				129	0.214	29.0	0.118	1.33	*
μ_ℓ = 0.90×10^{-3} Pa·s				173	0.285	30.5	0.129	1.40	*
Re_h = 2460				345	0.570	36.5	0.149	1.67	*
				518	0.854	42.0	0.170	1.93	*
				690	1.14	46.0	0.193	2.11	*
				863	1.42	47.1	0.204	2.16	*

(5) $Q_{\ell h}$ = 150 ℓ/min, $V_{\ell ho}$ = 1.12 m/s

$Q_{\ell v}$ (ℓ/min)	$V_{\ell v}$ (m/s)	f	$V_{\ell h}$ (m/s)	Q_{gv} (ℓ/min)	V_{gv} (m/s)	ΔP_h (mmH_2O)	f	C_D	
15	0.0248	5.39	0.208	43.2	0.0712	14.0	0.069	0.63	*
				86.3	0.142	19.7	0.087	0.89	*
T_ℓ = 29 °C				129	0.214	25.2	0.103	1.15	*
μ_ℓ = 0.81×10^{-3} Pa·s				173	0.285	27.6	0.121	1.25	*
Re_h = 2740				345	0.570	35.7	0.140	1.61	*
				518	0.854	39.6	0.162	1.79	*
80	0.132	5.06	0.221	43.2	0.0712	14.1	0.065	0.56	*
				86.3	0.142	20.1	0.084	0.81	*
T_ℓ = 34 °C				129	0.214	22.3	0.096	0.89	*
μ_ℓ = 0.74×10^{-3} Pa·s				173	0.285	24.3	0.109	0.97	*
Re_h = 3200				345	0.570	34.2	0.135	1.37	*
				518	0.854	38.0	0.152	1.53	*
150	0.248	4.16	0.269	86.3	0.142	18.6	0.085	0.50	*
T_ℓ = 37 °C				129	0.214	23.4	0.099	0.63	*
μ_ℓ = 0.7×10^{-3} Pa·s				173	0.285	22.5	0.108	0.61	*
Re_h = 4120				345	0.570	30.3	0.132	0.82	*

Table A-5 Two-phase cross flow test results
(Slit width = 120 mm, Attack angle = 60°)

$Q_{\ell v}$ = 80 ℓ/min, $V_{\ell v}$ = 0.104 m/s

$Q_{\ell h}$ (ℓ/min)	$V^{in}_{\ell h}$ (m/s)	Q_{gv} (ℓ/min)	V_{gv} (m/s)	ΔP_h (mmH_2O)	α	C^o_D (1/m)
50	0.0809	(22)	(0.028)	9.7	0.062	203
		(35)	(0.045)	13.6	0.093	285
T_ℓ = 10 °C		43.2	0.056	14.6	0.113	306
		64.7	0.084	16.3	0.128	342
		86.3	0.112	17.0	0.143	357
		108	0.140	17.0	0.164	357
		129	0.167	16.7	0.179	350
		173	0.224	14.1	0.218	296
		345	0.446	13.6	0.304	285
		518	0.670	19.9	0.373	417
		863	1.12	19.9	0.420	417
100	0.162	(22)	(0.028)	18.3	0.063	96
		(34)	(0.044)	23.5	0.090	123
T_ℓ = 20 °C		(47)	(0.061)	25.9	0.116	136
		86.3	0.112	30.0	0.137	157
		129	0.167	34.7	0.164	182
		173	0.224	38.3	0.182	201
		173	0.224	38.4	0.203	201
		345	0.446	46.2	0.239	242
		518	0.670	51.0	0.299	267
		898	1.16	58.2	0.389	305
		1290	1.67	Oscillation	0.442	——

Table A-6 Two-phase cross flow test results
(Slit width = 120 mm, Attack angle = 45°)

$Q_{\ell v}$ = 80 /min, $V_{\ell v}$ = 0.105 m/s

$Q_{\ell h}$ (ℓ/min)	$V_{\ell h}^{in}$ (m/s)	Q_{gv} (ℓ/min)	V_{gv} (m/s)	ΔP_h (mmH_2O)	α	C_D^o (1/m)
30	0.0485	(26)	(0.034)	1.4	0.055	82
		43.2	0.057	5.5	0.084	320
T_ℓ = 24 °C		86.3	0.113	6.8	0.167	396
		129	0.169	4.0	0.207	233
		173	0.227	3.3	0.225	192
		345	0.453	(1.0)	0.317	——
50	0.0809	(30)	(0.039)	2.18	0.02	46
		43.2	0.057	5.44	0.056	114
T_ℓ = 10 °C		86.3	0.113	11.9	0.087	250
		129	0.169	12.6	0.142	264
		173	0.227	10.7	0.174	224
		345	0.453	5.44	0.278	114
		518	0.679	minus	0.362	——
100	0.162	(30)	(0.039)	5.44	0.035	29
		43.2	0.057	10.5	0.075	55
T_ℓ = 16 °C		86.3	0.113	16.0	0.089	84
		129	0.169	21.1	0.118	111
		173	0.227	24.3	0.138	127
		345	0.453	28.6	0.173	150
		518	0.679	31.9	0.224	167
		863	1.13	37.4	0.282	196
		1290	1.69	Oscillation	0.311	——